Title

Emissions of trace gases and aerosols during the open combustion of biomass in the laboratory

Author

McMeeking, Gavin R.

Publication Date

2009-08-24

Emissions of trace gases and aerosols during the open combustion of biomass in the laboratory

Gavin R. McMeeking[1,2*], Sonia M. Kreidenweis[1], Stephen Baker[3], Christian M. Carrico[1], Judith C. Chow[4], Jeffrey L. Collett, Jr.[1], Wei Min Hao[3], Amanda S. Holden[1], Thomas W. Kirchstetter[5], William C. Malm[6], Hans Moosmüller[4], Amy P. Sullivan[1], and Cyle E. Wold[3]

[1]Department of Atmospheric Science, Colorado State University, Fort Collins, Colorado, USA

[2]Now at Center for Atmospheric Science, University of Manchester, Manchester, UK

[3]Fire Sciences Laboratory, United States Forest Service, Missoula, Montana, USA

[4]Division of Atmospheric Sciences, Desert Research Institute, Nevada System of Higher Education, Reno, Nevada, USA

[5]Environmental Energy Technologies Division, Lawrence Berkeley National Laboratory, Berkeley, California, USA

[6]National Park Service/CIRA, Colorado State University, Fort Collins, Colorado, USA

*To whom correspondence should be addressed, gavin.mcmeeking@manchester.ac.uk

Submitted to: Journal of Geophysical Research – Atmospheres

15 May 2009

ABSTRACT

We characterized the gas- and speciated aerosol-phase emissions from the open combustion of 33 different plant species during a series of 255 controlled laboratory burns during the Fire Laboratory at Missoula Experiments (FLAME). The plant species we tested were chosen to improve the existing database for U.S. domestic fuels: laboratory-based emission factors have not previously been reported for many commonly-burned species that are frequently consumed by fires near populated regions and protected scenic areas. The plants we tested included the chaparral species chamise, manzanita, and ceanothus, and species common to the southeastern US (common reed, hickory, kudzu, needlegrass rush, rhododendron, cord grass, sawgrass, titi, and wax myrtle). Fire-integrated emission factors for gas-phase CO_2, CO, CH_4, C_{2-4} hydrocarbons, NH_3, SO_2, NO, NO_2, HNO_3 and particle-phase organic carbon (OC), elemental carbon (EC), SO_4^{2-}, NO_3^-, Cl^-, Na^+, K^+, and NH_4^+ generally varied with both fuel type and with the fire-integrated modified combustion efficiency (MCE), a measure of the relative importance of flaming- and smoldering-phase combustion to the total emissions during the burn. Chaparral fuels tended to emit less particulate OC per unit mass of dry fuel than did other fuel types, whereas southeastern species had some of the largest observed EF for total fine particulate matter. Our measurements often spanned a larger range of MCE than prior studies, and thus help to improve estimates for individual fuels of the variation of emissions with combustion conditions.

INDEX TERMS

aerosols and particles (0305), constituent sources and sinks (0322), geochemical cycles (0330), pollution: urban and regional (0345), biogeochemical cycles (0414), biosphere/atmosphere

interactions (0315)

1. INTRODUCTION

Biomass burning emissions are a significant, global source of trace gas and aerosol species in the atmosphere and affect climate, visibility and human health [*Crutzen and Andreae*, 1990; *Naeher et al.*, 2007; *Watson*, 2002]. Although biomass burning emissions in the continental United States have been estimated to represent only ~5% of annual average global emissions (computed for 1997-2004) [*van der Werf et al.*, 2006], they play a large role in U.S. urban and regional air quality, including visibility [*McMeeking et al.*, 2006; *Park et al.*, 2006; *Park et al.*, 2007; *Phuleria et al.*, 2005; *Robinson et al.*, 2006]. For example, *Park et al.* [2007] estimated that biomass burning contributed about 50% of the annual mean total particulate carbon (TC) concentrations across the continental U.S., with summer wildfires identified as the most important driver of interannual variability in observed TC concentrations [*Spracklen et al.*, 2007]. Further, it is expected that the frequency and magnitudes of wildfires will increase in coming decades in regions affecting the U.S. [*Spracklen et al.*, 2007], which, along with increased demand for prescribed burning to reduce fuel loads in vulnerable regions [e.g., *Haines et al.*, 2001], will result in increasing impacts from biomass burning.

Model estimates of fire emissions and their impacts require not only burned-area and fuel loading inventories, but also fuel-based emission factors (EF) for both gaseous and particulate phase emissions. Emission factors relate the mass of a chemical species emitted to the mass of fuel burned [e.g., *Park et al.*, 2007; *Schultz et al.*, 2008; *Wiedinmyer et al.*, 2006]. EF have been measured in the laboratory and in the field for at least the last 40 years, but they remain a significant source of uncertainty in regional and global estimates of fire emissions [*Schultz et al.*, 2008; *Wiedinmyer et al.*, 2006]. Most EF measurements have concentrated on fuels from regions outside of the continental U.S., since these account for the largest fractions of global emissions and thus have the most significant impacts on global tropospheric chemistry. *Andreae and Merlet* [2001] conducted an extensive literature review and compiled recommended EFs for three primary ecosystem types: savanna and grassland, tropical forests, and extratropical forests. These EFs have been applied in many modeling studies [e.g., *van der Werf et al.*, 2006]. Although *Andreae and Merlet* [2001] included North American fuels in their survey, the recommended average values do not necessarily reflect the specific fuel types and combustion conditions most important at U.S. local and regional scales.

Battye and Battye [2002] summarized much of the work reported in the peer-reviewed and grey literature that applied to emissions from U.S. wildland fires, with a focus on field studies, primarily airborne, of emissions from fires in forested regions in the northwestern US. and Alaska, as well as chaparral fires and fires in the southeastern U.S. [*Cofer et al.*, 1988a; *Cofer et al.*, 1988b; *Friedli et al.*, 2001; *Hardy et al.*, 1996; *Hays et al.*, 2002; *Muhle et al.*, 2007; *Yokelson et al.*, 1999]. While field studies have the advantage of measuring emissions from an actual fire, as pointed out by *Yokelson et al.* [2008], they offer only a snapshot in time, space, and combustion phase, and the number of measured species is limited. Controlled laboratory studies can be used to fill in some of these gaps. Some recent laboratory studies of U.S.-relevant fuels have been conducted [*Chakrabarty et al.*, 2006; *Chen et al.*, 2006; *Chen et al.*, 2007; *Hays et al.*, 2002], but we are unaware of published laboratory measurements of emissions from individual chaparral or southeastern U.S. plant species. Earlier laboratory wind-tunnel studies examining several Californian fuels were primarily focused on agricultural waste [*Jenkins et al.*, 1991; *Jenkins et al.*, 1993; *Jenkins et al.*, 1996; *Turn et al.*, 1997]. There have been a number of studies focusing on characterization of source profiles, used for source apportionment estimates, for fuels commonly consumed by residential fireplace or wood stove burning, because of their role in urban and suburban air quality degradation [*Fine et al.*, 2001; 2002a; b; 2004; *Lipsky and Robinson*, 2006; *Roden et al.*, 2006]. Finally, very few studies have presented a comprehensive set of measurements that include both gas-phase and speciated particulate-phase emissions, along with an indicator of combustion conditions.

The Fire Laboratory at Missoula Experiment (FLAME) aimed to fill some of the gaps in available data on emissions from fires in the U.S. The study took place at the US Forest Service's Fire Sciences Laboratory (FSL) in 2006 (FLAME 1) and 2007 (FLAME 2). Earlier experiments performed at the FSL examined fire combustion behavior [*Freeborn et al.*, 2008], trace gas emissions [*Christian et al.*, 2004; *Goode et al.*, 1999; *Yokelson et al.*, 1996; *Yokelson et al.*, 1997] and aerosol emissions [*Chakrabarty et al.*, 2006; *Chen et al.*, 2006; *Chen et al.*, 2007; *Engling et al.*, 2006; *Freeborn et al.*, 2008]. FLAME expanded on this work by including additional fuels and fuel components most relevant to wildland fire and prescribed burning in the U.S., and adding/improving measurements of aerosol properties, including emissions of smoke marker species [*Sullivan et al.*, 2008], mercury compound emissions [*Obrist et al.*, 2008], particle size distributions and refractive index [*Levin et al.*, in preparation], aerosol hygroscopicity, cloud condensation nuclei (CCN) and ice nuclei (IN) activity [*Petters et al.*, 2009], and aerosol optical properties [*Lewis et al.*, 2008; *Mack et al.*, in preparation].

2. FUEL SELECTION AND TREATMENT

Leaves and woody material from 33 unique plant species (Table 1) were burned individually and in various combinations during FLAME 1 and 2. Fuels that were too moist to burn were dried at 35°-40° C for 48–72 hours. The remaining untreated fuels had dried sufficiently during shipping and storage to be used without drying. Fuel moisture (FM, dry weight percent; see Table S1) for each fuel as used was determined by holding a sample at 100° C for 48 hours and measuring the mass loss. Fuel carbon and nitrogen contents (Table 1) were measured by an independent laboratory. We selected fuels based on their modeled frequency of consumption in wild- and prescribed fires in the western and southeastern United States and in fire-impacted regions in close proximity to urban areas. We further prioritized selection of species for which little or no peer-reviewed, controlled laboratory emissions data were available.

2.1. Chaparral

Chaparral is a highly diverse ecosystem that is distributed from Baja California to south-central Oregon and covers approximately 6% of the area of California [*Keeley and Davis*, 2007]. Chaparral-dominated regions coincide with many highly populated areas in California, most notably the Los Angeles and San Diego metropolitan regions, underscoring the need for accurate emission inventories for chaparral fuels. For example, *Clinton et al.* [2006] estimated that ~80% of the fuel consumed by a series of major wildfires in southern California during 2003 were shrubs and duffs. The dominant species within the chaparral ecosystem include chamise (*Adenostoma fasciculatum*) and species in the *Ceanothus* and *Arctostaphylos* genera [*Keeley and Davis*, 2007]. We tested three fuels representing this ecosystem: chamise, hoaryleaf ceanothus (*Ceanothus crassiofolis*), and Eastwood's manzanita (*Arctostaphylos glandulosa*). Samples were collected from the San Jacinto Mountains, about 150 km east of Los Angeles, California (see Table 1). Chaparral fire emissions have been observed from aircraft [*Cofer et al.*, 1988a; *Cofer et al.*, 1988b; *Hegg et al.*, 1987], but we are unaware of laboratory measurements that have appeared in the peer-reviewed literature.

2.2. Montane and subalpine forests

Montane and subalpine coniferous forests cover major portions of the Sierra Nevada and

Cascade mountain ranges [*Fites-Kaufman et al.*, 2007], inland regions of the northwestern U.S. [*Franklin*, 1988], and northern Rocky Mountains [*Peet*, 1988]. This region encompasses many federal Class I areas that are protected against visibility degradation. Species from this ecosystem tested during FLAME included: ponderosa pine (*Pinus ponderosa*), logdepole pine (*Pinus cortata*), and Douglas-fir (*Pseudotsuga menziesii*). We burned needles, woody material, combinations of needles and woody material, as well as litter (dead needles and cones from the forest floor) and duff (partly decayed litter including a portion of the uppermost layers of soil). These species were collected from several rural locations near Missoula, Montana. We also burned a mixture of unidentified grass species collected from a site near the FSL.

2.3. Rangeland

Sagebrush rangeland ecosystems are one of the most widespread in the intermountain west, primarily found in eastern Oregon, southern Idaho, Nevada and Utah [*West and Young*, 2000]. In addition to big sagebrush (*Artemisia tridentate*), we also burned two other woody species found from this region: Gray's rabbitbrush (*Chrysothamnus nauseosus*) and Utah juniper (*Juniperus osteosperma*). The rabbitbrush and juniper samples were collected near Salt Lake City, Utah. Sagebrush samples were collected from two other areas: an urban setting near the Salt Lake City airport and a rural setting near Missoula, Montana.

2.4. Southeastern coastal plain

Forest, rangeland and cropland undergo prescribed burning each year in the southeastern U.S. [*Haines et al.*, 2001], but wildfires also occur in this region. We burned several species common to the coastal plain region of the southeastern U.S., including longleaf pine (*Pinus palustris*), and understory shrubs such as saw palmetto (*Serenoa repens*), gallberry (*Ilex gllabra*), and wax myrtle (*Myrica cerifera*). During periods of prolonged drought, fire can spread to dry savannah and wetland ecosystems, so we selected several representative species including titi (*Cyrilla racemiflora*), sawgrass (*Cladium mariscus*), common reed (*phragmites australis*), wiregrass (*Aristida beyrichiana*) and black needlerush (*Juncus roemerianus*). We also burned kudzu (*Pueraria lobata*), an invasive species that is frequently the target of control efforts, which include prescribed burning.

2.5. Boreal forests

Boreal forest fires are a major source of carbon to the atmosphere [*Kasischke et al.*, 1995], and their emissions have major impacts on the atmosphere on local and global scales [e.g., *French et al.*, 2002; *O'Neill et al.*, 2002; *Pfister et al.*, 2008; *Stohl et al.*, 2006; *Trentmann et al.*, 2006]. Emissions from boreal North America alone accounted for ~10% of annual average global emissions from 1997-2004 [*van der Werf et al.*, 2006] and have been observed to be transported into the U.S. [e.g., *Al-Saadi et al.*, 2005]. White spruce (*Picea glauca*) and black spruce (*Picea mariana*) are ubiquitous conifer species in boreal forests and are commonly found in spruce-feathermoss forests that dominate the southern boreal forest zone, which includes a large portion of Alaska [*Elliot-Fisk*, 1988]. We burned spruce samples collected within ~50 km of Fairbanks, Alaska. Wildfires and prescribed burns affect belowground biomass in addition to shrubs and trees, so we also burned samples taken from forest floor (duff), which consists of the uppermost layer of soil with live and dead feathermoss (*Pleurozium schreberi*). However, we note that we did not have any samples of the underlying peat below the surface duff, which can contribute substantially to total fire emissions [*Kasischke et al.*, 2005; *Yokelson et al.*, 1997].

2.6. Other fuels

We included a mixture of plants that are frequently burned in Puerto Rico, as biomass burning emissions from this region, as well as from Mexico and Central America, can be transported to the southeastern U.S. [*Kreidenweis et al.*, 2001]: teak (*Tectona grandis*), sea hibiscus (*Hibiscus tiliaceus*), peltophorum (*Peltophorum inerme*), sacky sac bean (*Inga laurina*), and fern (*Decranopteris pectinata*). Two agricultural waste products that are burned after harvest were collected in Asia: rice straw (*oryza sativa)* from Taiwan and sugar cane (*saccharum officenarum*) from the Guangdong province of China. Although outside the scope of our general focus on U.S. inventories, emissions from these agricultural wastes have attracted recent interest [*Christian et al.*, 2003; *Yokelson et al.*, 2008] and have been shown to affect air quality in populated regions [*Viana et al.*, 2008; *Yang et al.*, 2006].

3. EXPERIMENTAL METHOD

3.1. Facility and burn procedure

The experiments were performed at the U.S. Forest Service's combustion testing facility at the Fire Sciences Laboratory in Missoula, Montana, which is depicted in Figure 1 and has been described previously [*Bertschi et al.*, 2003; *Christian et al.*, 2003; *Yokelson et al.*, 1996; *Yokelson et al.*, 2008]. The main combustion chamber is a square room with internal dimensions 12.4 x 12.4 x 19.6 m high with a total volume of ~3000 m^3. Outside air was conditioned for temperature and humidity and pumped into the chamber prior to each burn. An exhaust stack located at the center of the room begins 2.1 m above the floor and extends through the chamber ceiling. An inverted funnel at the bottom of the exhaust stack narrows from a 3.6 m diameter opening to the 1.6 m stack diameter [*Christian et al.*, 2003]. Sampling ports that originate near the center of the flow and pass through the walls of the exhaust stack are located ~16.5 m above the floor, and are accessed from a measurement platform near the ceiling.

Two types of experiments were performed during FLAME, which we refer to as 'stack' and 'chamber' burns (Table S1). During stack burns, emissions from the fuel bed, located directly beneath the inverted funnel, were drawn through the exhaust stack. Instruments located on the measurement platform continuously sampled through the platform sample ports. *Christian et al.* [2004] used direct observations of gas profiles to confirm that emissions are well-mixed across the stack. In contrast, the combustion room was sealed during chamber burns by closing the exhaust stack. The fuel bed was placed about halfway between the exhaust stack and the chamber wall and a large circulation fan operated in one corner to facilitate mixing. Continuous-sampling instruments were relocated from the measurement platform to laboratories adjacent to the combustion chamber, and drew samples through wall ports. Chamber burns were designed primarily for optical closure experiments not reported here, as those measurements required lower species concentrations and longer sampling periods (~2 hours) compared to those possible during stack burns, which typically lasted from five to ten minutes.

The majority of samples burned during stack experiments were placed on a 46 x 61 cm horizontal metal tray covered with an inert ceramic heat shield. Fuels were stacked horizontally on the fuel bed to facilitate ignition, except for two large fuel mass burns (~2500 g) when fuels were stacked in a cylindrical wire cage. The fuel bed was placed on a Mettler-Toledo PM34 balance to monitor its mass as a function of burn time. The initial fuel mass (m_0) and final residual mass ($m_{residual}$), both listed in Table S1 for each burn, were measured with a higher sensitivity PM34-K balance (Mettler-Toledo). Initial fuel masses ranged from 25 to 2500 g depending on the objective of the experiment and desired emission concentrations; most were between 100 and 250 g.

We ignited the fuel bed using several methods. During FLAME 1, dry fuels were ignited using a butane pilot lighter applied briefly to the edge of the fuel bed. Fuels with high fuel moistures required the application of a propane torch or heated metal coils for a significant period of time, in some cases continuously, to maintain the fire. Both ignition methods often resulted in a propagating flame front that moved through the fuel bed and simultaneous flaming and smoldering combustion in different parts of the fuel bed. We modified the fuel bed in the FLAME 2 experiments [*Sullivan et al.*, 2008]. Fuels were placed on a lattice of heating tape that was soaked with ~15 g of ethanol, which was vaporized and ignited on heating, uniformly igniting the fuel bed. The dense duff core samples still required application of the propane torch to sustain combustion, but all other fuels were ignited effectively using this method. Table S1 provides the components of the plant or plants that were burned during each burn, the ignition method, and the fuel moisture content. We performed three replicate burns for each fuel type during FLAME 1 stack burns and two replicate stack burns during FLAME 2.

3.2. Real-time gas measurements

Real-time measurements of CO_2, CO, NO, and NO_2 were made at ~2 second resolution using three commercial gas analyzers, sampling through aluminum (C gas analyzers) or Teflon lines (NO_x analyzer). Carbon dioxide and water vapor mixing ratios were measured by a Li-Cor Model 6262 non-dispersive infrared gas analyzer. Carbon monoxide mixing ratios were measured using a Thermo Environmental Model 48C variable-range gas filter correlation analyzer. Two sets of mixed standards ($[CO_2]$ = 362 ppm, [CO] = 0.5 ppm and $[CO_2]$ = 499 ppm, [CO] = 2.7 ppm) were passed through the analyzers prior to burn ignition for calibration. The mixing ratios of nitrogen oxides ($NO_X = NO + NO_2$) were measured by a Thermo Environmental Model 42 chemiluminescence analyzer. We observed high (>2000 ppb) NO_X concentrations that saturated the analyzer during several FLAME 2 burns and do not report those NO_X data. In some of those cases the NO measurement was valid and is reported. The estimated accuracy/precision of the measurements were: Li-Cor, 1%/0.1%; TECO, 2%/1%.

3.3. Trace gas canister measurements

Canister samples of emissions drawn directly from the stack and chamber were analyzed for CO_2, CO, CH_4 (methane), C_2H_4 (ethene), C_2H_6 (ethane), C_3H_6 (propene), C_3H_8 (propane), three isomers of C_4H_8 (butene), and C_4H_{10} (n-butane) gases with a Hewlett Packard model 5890 Series II gas chromatograph. Background samples were collected in several canisters throughout the day during the experiments and used to calculate the excess mixing ratios of each measured species (e.g., $\Delta CH_4 = CH_{4,\text{ measured}} - CH_{4,\text{ background}}$). The CO_2 and CO analyses use a 1 mL sample loop to inject the sample, and a 1/8" diameter x 6 foot Carbosphere (Alltech) column to separate CO_2, CO, and air with a helium carrier gas at a flow rate of 16 mL min^{-1}. After separation in the column the sample enters a nickel catalyst methanizer (375° C), which converts the CO_2 and CO to CH_4, and then a flame ionization detector (FID) at 350° C. The oven temperature program is isothermal at 100° C. The C_1-C_4 analyses are performed using a 0.25 mL sample loop, with a 0.53 mm x 30 m GS-Q (J&W Scientific) column with a helium carrier gas at 6 mL min^{-1}. The oven temperature program for this analysis is 30° C for 6 minutes, then increasing by 10° C min^{-1} to a final temperature of 90° C for 8 minutes.

Chromatogram data were processed by Hewlett Packard ChemStation II software. A set of gas standards bracketing the sample concentrations were analyzed with each set of samples to construct a standard curve for each compound. Based on the integrated peak areas, the sample concentrations were calculated from the standard curves. Duplicate analyses were performed every sixth sample to quantify measurement precision error. National Institute of Standards and Technology (NIST) primary standards of CO_2, CO, and CH_4 were analyzed as samples to measure overall accuracy. Accuracies/uncertainties in the GC analyses are 1%/1% for CO_2, CO, and CH_4, and 10%/10% for $C_{2\text{-}4}$ gases.

3.4. Trace gas denuder measurements

We measured ammonia (NH_3), nitric acid (HNO_3), and sulfur dioxide (SO_2) concentrations emitted from fires using annular denuders (URG Corporation, Chapel Hill, NC). The denuders operated in series with a filter sampling system (see Section 3.5). The sample flow was nominally 10 L min^{-1} and was pulled through a Teflon-coated inlet; *Brauer et al.* [1989] cite efficiencies of 97.3-98.5% for sampling of NH_3 through similar inlets. The HNO_3 denuder was coated with 10 mL of a 1% sodium carbonate + 1% glycerol in a 1:1 methanol/water solution and the NH_3 denuder was coated with 10 mL of a 1% phosphorous acid in a 9:1 methanol/water solution [*Perrino et al.*, 1990; *Perrino and Gherardi*, 1999]. Coated denuders were dried with N_2 for ~10 minutes. After sampling, each denuder was extracted using 10 mL of deionized water. Extracts were analyzed using a Dionex DX-500 series ion chromatograph. Details of the analysis procedure are given by *Yu et al.* [2006] and *Lee et al.* [2008]. Minimum detection limits (MDL) for each species were determined from blank samples and values below the MDL are not reported.

3.5. Particulate filter samplers

Three types of filter samplers collected particulate matter on filters during the burns for compositional analysis: a URG annular denuder/filter sampling system (URG, Chapel Hill, North Carolina), a high-volume sampler (Hi-vol; Thermo Anderson, Smyrna, Georgia), and two IMPROVE (Interagency Monitoring of Protected Visual Environments) samplers [*Malm et al.*, 2004]. The Hi-vol and URG samplers were located on the sampling platform during stack burns. During chamber burns, they were moved to the chamber floor, with the Hi-vol samplers on tables to keep the inlets of both samplers at a uniform height (~3 m). The IMPROVE samplers had inlets at a similar height, and only ran during chamber burns because of space restrictions on the stack sampling platform. During stack burns, the filter sampler pumps were turned on 30 seconds prior to ignition and turned off when the fire was considered extinguished based on visual observations. During chamber burns, the filter sampler pumps were started approximately four minutes after ignition, and individual aerosol samples for each burn were typically collected over two hours.

The Hi-vol sampler collected sample on quartz filters for thermal optical OC/EC analysis. *Sullivan et al.* [2008] and *Engling et al.* [2006] described the Hi-vol sampler we used during FLAME. The sampler had a nominal flow rate of 1.13 m^3 min^{-1}. An assembly of two quartz-fiber filters collected particles divided into two size classes: those with aerodynamic diameters (D_{ae}) > 2.5 μm (coarse mode) and those with D_{ae} < 2.5 μm (fine mode). We only present results from the analysis of the 20.3 x 25.4 cm fine mode filter—equivalent to particulate matter (PM) with D_{ae} < 2.5 μm or $PM_{2.5}$—because an examination of the IMPROVE filters and volume size distributions [*Levin et al.*, in preparation; *Sullivan et al.*, 2008] confirmed that total aerosol mass was dominated by particles in the sub-2.5 μm diameter size range, as expected [e.g., *Ward and Hardy*, 1991]. The quartz filters were wrapped in aluminum foil and baked in an oven over a 36 hour period (12 hour heating at 550° C + 24 hour cool down) prior to sampling to remove any organic contaminants. Punches from the hi-vol filters were analyzed for the masses of carbon in the OC and EC fractions with a semi-continuous analyzer (Sunset Laboratory, Tigard, Oregon) in 'off-line' mode [*Sullivan and Weber*, 2006]. The OC/EC measurements reported here were the average of two 1.4 cm^2 punches from the same filter to reduce measurement uncertainties associated with sample loading heterogeneity [*Gorin et al.*, 2006].

The URG sampling system consisted of two annular denuders and a filter pack arranged in series, which collected aerosol samples for ion chromatography (IC) analysis [*Lee et al.*, 2004]. The 10 lpm sample flow first passed through a Teflon-coated 2.5 μm size cut cyclone to remove large particles, and then through two denuders (Section 3.4) and a nylon filter (Gelman Nylasorb, 1.0 μm pore size). A backup cellulose filter coated in citric acid collected any NH_3 lost from the particles collected on the nylon filter. The URG filters were extracted using 6 mL of deionized water. Extracts were analyzed for inorganic species (Cl^-, SO_4^{2-}, NO_3^-, Na^+, NH_4^+, K^+, Mg^{2+}, and Ca^{2+}) using two Dionex DX-500 IC systems.

Particles were also collected by two IMPROVE sampling systems during the chamber burns, slightly modified from those used in the IMPROVE network [*Malm et al.*, 2004]. Each system had only A, B and C modules, holding Teflo, Nylasorb, and quartz filters, respectively, and collected particulate matter after $PM_{2.5}$ or PM_{10} inlets. The C modules held two quartz filters in series to characterize organic aerosol sampling artifacts. During several FLAME 1 burns, the IMPROVE modules operated for different time intervals than the other samplers; in those cases smoke species concentrations were corrected using measurements of the room air background concentrations and the total time that room air was sampled. Gravimetric mass was measured from Module A filters following the standard procedure used for samples collected in the IMPROVE network, with relative humidity in the weighing laboratory maintained between 20–40%.

3.6. Organic and elemental carbon thermal optical analysis (TOA) protocols

The OC and EC measurements presented here were obtained using two different protocols. Samples collected by the IMPROVE sampler were analyzed using the IMPROVE_A analysis protocol [*Chow et al.*, 2007], in which the sample is heated to four temperature plateaus (140, 280, 480 and 580 °C) in pure helium and three temperature plateaus (580, 740 and 840 °C) in 98% helium and 2% oxygen. Analysis of the hi-vol punches using the Sunset analyzer followed a modification of the NIOSH 5040 protocol [*Bae et al.*, 2004; *Birch and Cary*, 1996]. The sample punch was heated in pure helium to 600 °C in 80 seconds and then to 840 °C in 90 seconds. The sample was cooled for 35 seconds and oxygen added to the analysis atmosphere (98% He, 2% O_2). Punches were then heated to 550 °C in 30 seconds, 650 °C in 45 seconds, and 850 °C in 90 seconds.

Figure 2 compares EC/TC ratios measured for the IMPROVE $PM_{2.5}$, IMPROVE PM_{10}, and hi-vol filter samples collected during FLAME. The good agreement between EC/TC ratios found for the IMPROVE PM_{10} and $PM_{2.5}$ samples (r^2 = 0.95, regression coefficient = 0.98) shows that the EC fraction of TC was similar in both. EC/TC ratios obtained by the same protocol for high EC/TC ratios were strongly correlated, but they disagreed within about a factor of two between protocols for samples with low EC/TC ratios, similar to the discrepancies found in biomass burning-impacted samples in previous studies [*Watson et al.*, 2005]. It is unclear which method provides a more accurate measure of the EC content of the aerosol. In the remainder of this work, we use the Hi-vol/NIOSH 5040/Sunset OC and EC measurements, simply because they are a more complete data set (available for both stack and chamber burns).

Filter-based carbonaceous aerosol measurements are prone to artifacts caused by gas-phase adsorption onto filter fibers (positive artifact) and volatilization of the sampled particle phase organic material (negative artifact) [e.g., *Kirchstetter et al.*, 2001; *Mader and Pankow*, 2001; *Turpin et al.*, 1994]. During FLAME, the IMPROVE $PM_{2.5}$ and IMPROVE PM_{10} samplers collected aerosol using front and back quartz filters arranged in series. Ideally, the mass of OC (adsorbed gases) measured on the back filter equals the mass of OC measured on the front filter that was due to adsorbed gases. Overall, adsorption artifacts during FLAME appeared to be relatively small (Figure 3). At high OC concentrations (> 100 $\mu g\ m^{-3}$), when presumably more semi-volatile material was in the particle phase, back filter OC was ~2–5% of the front filter OC. At lower OC concentrations (< 50 μg m^{-3}), when more semi-volatile material should be in the gas phase, back filter OC approached 20% of the front filter OC, closer to the 20-50% values reported by *Fine et al.* [2001] and *Lipsky and Robinson* [2005; 2006]. In those studies, the aerosol samples were diluted to lower concentrations than we sampled during FLAME, which may have altered the partitioning of semi-volatile species toward the gas phase.

3.7. Emitted and consumed mass calculations

For the canister and denuder measurements, the total emitted mass of each species was computed from the product of the excess mixing ratios and the sample volume. The canister and denuder samplers operated throughout each stack burn and represent fire-integrated emissions. The continuous measurements of CO and CO_2 during chamber burns showed that the concentrations of these species did not vary significantly after the chamber became well mixed, within 30 minutes of ignition. The canisters were used to grab a sample from the chamber approximately 60 minutes into the experiment.

During the stack burns, filter and denuder samples were collected over multiple, replicate burns to ensure adequate concentrations for compositional analysis, particularly trace organic species [*Sullivan et al.*, 2008]. We usually sampled three replicate burns on a single filter during FLAME 1 and two replicate burns on a single filter during FLAME 2. To calculate emission factors for each aerosol species, we multiplied the mass concentrations of each species determined from the filter measurements by the total volume of air sampled through the stack. We calculated the mass of aerosol species emitted during the chamber burns by multiplying mass concentrations determined from filter measurements by the total volume of the chamber. This assumes that the emissions were well mixed, and therefore the calculations of emission factors for chamber burns have higher uncertainty than those for stack burns.

The mixing ratio measurements from the real-time gas analyzers were multiplied by the volume flux of air through the stack and integrated over the lifetime of the burn to obtain the total mass of CO, CO_2 and NO_X emitted during the stack burns. For chamber burns, we calculated the average gaseous-species mixing ratios for the period from 30 to 35 minutes following ignition, and multiplied by the chamber volume.

We adjusted the total mass of CO and CO_2 emitted for burns that used the ethanol-coil ignition system by subtracting the mean of the total emissions for each species during the two ethanol-coil test burns (0.13 g CO, 12.5 g CO_2). In general, the mass of plant material burned was 5-10 times greater than the mass of ethanol consumed during the ignition procedures. Exceptions were burns featuring low fuel masses conducted during FLAME 2 chamber burns. Emission data for burns that used the propane torch ignition method were adjusted by subtracting the total torch emissions, which were determined by multiplying the time the torch was on by the species emission rate. Burns that required the torch to be applied to maintain combustion for a period greater than half of the total burn time are omitted in the analyses.

The mass of dry biomass consumed (m_{consumed}), assuming the residual material contains no water, was calculated as:

$$m_{consumed} = \frac{m_{fuel}}{1 + FM} - m_{residual} \qquad 1$$

where FM is the fuel moisture fraction, m_{fuel} is the initial (wet) fuel mass and m_{residual} is the mass of ash and unburned fuel remaining. The carbon consumed (C_{consumed}) during each burn was calculated by multiplying m_{consumed} by x_c (Section 3.9).

3.8. Modified combustion efficiency calculation

Since biomass burning emissions are known to depend on the combustion conditions, it is useful to include a measure of the combustion efficiency in reporting observations. We adopt the approach used in many prior studies [e.g., *Yokelson et al.*, 2008] and report the fire-integrated modified combustion efficiency, MCE, which depends on the molar ratio of the emitted CO and CO_2 [*Ward and Radke*, 1993]:

$$MCE = \frac{\Delta[\mathrm{CO_2}]}{\Delta[\mathrm{CO}] + \Delta[\mathrm{CO_2}]} \qquad 2$$

where $\Delta[CO_2]$ and $\Delta[CO]$ are the fire-integrated excess molar mixing ratios of CO_2 and CO. To compute the excess quantities, we assumed the ambient concentrations of CO and CO_2 were equal to their mean values measured in the stack or chamber immediately prior to ignition (usually from 120 to 10 seconds before ignition). For stack burns, we determined the fire-integrated MCE for each burn by dividing the total mass of CO_2 (in g C) emitted by the net mass of CO_2 plus CO emitted, also in g C. For chamber burns, we computed the mean fire-integrated MCE during the 5-minute period between 30 and 35 minutes following ignition, as was done for other gases (Section 3.7). Table S1 lists the fire-integrated MCE for each burn.

3.9 Emission ratios and emission factors

Fire-integrated emission factors were calculated using the carbon mass balance (CMB) approach [*Ward and Radke*, 1993], in which the concentrations of emitted carbon-containing species are a proxy for the mass of dry fuel consumed during the fire. The emission factor for species *i* emitted by a fuel with carbon mass fraction (x_c) of the dry fuel mass is given by:

$$EF_i = \frac{m_i}{\mathrm{CO} + \mathrm{CO_2} + \mathrm{PM_C} + \Sigma\mathrm{HC}} x_c \qquad 3$$

where m_i is the mass of species *i* emitted, PM_C is the mass of particulate-phase carbon and ΣHC is the sum of the total mass of C contained in gas-phase hydrocarbons, estimated during FLAME as the sum of the measured $C_{1\text{-}4}$ hydrocarbons. We used the measured values of dry fuel mass x_c reported in Table 1 or assumed a value of 0.45 [*Andreae and Merlet*, 2001] in the absence of fuel carbon information. To report gas-phase emission factors on a burn-by-burn basis we must ignore the PM_c term in Equation 3, but it is usually a small fraction of the carbon emissions [*Lipsky and Robinson*, 2006] and, together with the contribution from carbon-containing gases not measured, causes an overestimation of EF on the order of only 1-2% [*Andreae and Merlet,* 2001]. All emission factors reported here are in units of g species per kg dry fuel, unless stated otherwise.

4. RESULTS

4.1. Fire behavior and combustion efficiency

Fire-integrated MCE values ranged from approximately 0.75–0.95, but we also observed MCE values outside this range for burns in which we only sampled flaming or smoldering phase emissions (see Table S1). Our best estimate of the variability in fire-integrated MCE for a single fuel was derived from 15 replicate ponderosa pine needle litter burns with constant FM (9.9 ± 0.5%) and initial fuel mass (246 ± 6 g), for which we calculated fire-integrated MCE values ranging from 0.88 to 0.94 with a mean and standard deviation 0.92 ± 0.02.

In some cases, fuels with higher FM tended to have lower fire-integrated MCE, indicating smoldering combustion contributed more to emissions than did flaming combustion, as might be expected (Figure 4). For example, untreated ponderosa pine needles (FM ~60%) had a fire-integrated MCE of 0.86 whereas dry ponderosa pine needles (FM ~10%) had a fire-integrated MCE of 0.94. However, factors other than FM affected MCE. We observed larger MCE values when we increased the mass of fuel while holding fuel moisture constant during a series of ponderosa pine needle burns. Burning different plant components also resulted in different combustion behavior; we observed higher MCE for chamise and Douglas fir woody material compared to leaves and needles.

4.2. Total particulate emissions

The gravimetric mass concentration data from the chamber burns confirmed that the PM_{10} mass concentrations were dominated by $PM_{2.5}$ mass concentrations (Figure 5). The PM_{10} to $PM_{2.5}$ mass ratio was 1.09, estimated from a zero-intercept linear regression of all but the three highest-concentration samples. The ratio increased to 1.16 if all samples were included in the regression. On average, aerosol emissions were dominated by carbon and TC made up almost 90% of reconstructed $PM_{2.5}$ mass emissions, which we computed by summing all identified aerosol species, as gravimetric data were only available for chamber burns:

$$\text{reconstructed PM}_{2.5} = \sum (\text{ionic species})_{\text{URG}} + EC + OC \times 1.5 \qquad 4$$

The rationale for the factor of 1.5 is discussed in Section 4.3.4. We observed a large range in fire-integrated $PM_{2.5}$ emission factors (1.9–82.1 g kg^{-1} fuel). Since OC dominated $PM_{2.5}$ and its emissions are higher in smoldering combustion, the $PM_{2.5}$ EF also depended on MCE. *Reid et al.* [2005] estimated fine aerosol emission factors of ~9 g kg^{-1} fuel based on flaming combustion measurements—which they define as MCE > 0.9—and ~34 g kg^{-1} fuel for smoldering combustion measurements (MCE < 0.9). *Yokelson et al.* [2008] obtained an average $EFPM_{2.5}$ of 9.93 g kg^{-1} dry fuel in their laboratory studies of tropical fuels, similar to the recommendation of *Reid et al.* [2005], with variations between 2.17 and 16.61 g kg^{-1} for various fuels that had fire-integrated MCEs between 0.88 and 0.979. *Ward and Hardy* [1991] recommended $EFPM_{2.5}$ of 10 g kg^{-1} for cured grasses, 15 g kg^{-1} fuel for chaparral and palmetto/gallberry fires and 20-50 g kg^{-1} for long-needled conifer fires. In FLAME, the average $EFPM_{2.5}$ for chaparral species was 11.6 ±

15.1 g kg^{-1} dry fuel; for palmetto, 11.4 ± 10.5 g kg^{-1} dry fuel; and for montane fuels (long-leaf conifers) 29.4 ± 25.1 g kg^{-1} dry fuel, on average, all very similar to previous recommendations.

4.3. Carbon species

4.3.1. Total carbon mass balance

We calculated the mass of carbon emitted (C_{emitted}) during each burn by adding together carbon emitted in the form of CO_2, CO, CH_4, $C_{2\text{-}4}$ hydrocarbons, and particle-phase OC and EC, for burns where all of these measurements were available. Figure 6 compares C_{emitted} to C_{consumed}, with the points coded by burn type and shaded by FM because the assumption of zero residual water content may not be valid for high moisture content fuels. The masses of carbon emitted and consumed were highly correlated (r^2 = 0.96) and close to the 1:1 line, indicating that emissions were effectively captured by the stack and could justifiably be assumed to be well-mixed in the chamber. On average, 89 ± 5.7% of the carbon was emitted in the form of CO_2, followed by CO (6.9 ± 3.0%), OC (2.3 ± 2.5%), C_2-C_4 hydrocarbons (1.3 ± 1.9%), CH_4 (0.5 ± 0.4%), and EC (0.2 ± 0.2%).

4.3.2. Carbon monoxide and carbon dioxide

We report fire-integrated emission factors for CO and CO_2 in Table S1 and emission factors averaged for each plant species and ecosystem classifications described in Section 2 in Table 2. The species and ecosystem data are the averages of all burns for that species or ecosystem type, so the numerical values depend on the number and variety of burns performed. The emission factors for many species are driven by the relative contributions from flaming and smoldering combustion during each burn, as expressed through fire-integrated MCE in this work, and the carbon abundance in the fuel. For example, Alaskan duff featured a strong contribution from smoldering combustion (average MCE = 0.867 ± 0.074), but had a lower CO emission factor than several fuels with higher average MCE because it contained less carbon per unit mass (Table 1).

The average $EFCO_2$ for montane fuels was 1552 ± 150 g kg^{-1} dry fuel (mean ± 1 standard deviation), near the 1569 ± 131 g CO_2 kg^{-1} dry fuel recommended by *Andreae and Merlet* [2001] for extratropical forests. The $EFCO_2$ for rangeland fuels was somewhat lower (1489 ± 176 g kg^{-1} dry fuel) and for coastal plain fuels was somewhat higher (1632 ± 150 g kg^{-1}), reflecting the different contributions from flaming and smoldering combustion quantified through the fire-integrated MCE. The average EFCO for montane fuels was 92 ± 34.1 g kg^{-1} dry fuel, somewhat lower than the value recommended by *Andreae and Merlet* [2001] for extratropical forests (107 ± 37 g kg^{-1} dry fuel). Rangeland and chaparral fuels had similar average EFCO as montane fuels, but the average coastal plain value was lower (78.0 ± 27.7 g kg^{-1} dry fuel), again reflecting different average contributions of flaming and smoldering combustion.

4.3.3. Gas-phase hydrocarbons

Fire-integrated emission factors for most of the measured hydrocarbon species were positively correlated with MCE, with coefficients of variation (r^2) ranging from 0.39–0.67. In Figure 7, we compare our results to the regressions reported by *Christian et al.* [2003] for emissions from grasses and several species from the African savanna, Indonesia and North American forests burned at the FSL. The FLAME and *Christian et al.* [2003] regressions for CH_4 were in nearly perfect agreement. The two studies took place in the same facility, but examined different fuels, and used a different method to determine CH_4 concentrations (gas chromatography versus open path FTIR). *Yokelson et al.* [2003] measured slightly higher emission factors for CH_4 over African savanna fires, but obtained a similar slope. A number of

FLAME samples fall on the *Yokelson et al.* [2003] regression, but it is unclear if this is just a coincidence or reflects a systematic difference in CH_4 emissions for different fuels or fire regimes. The FLAME emission factors for C_2H_2 and C_2H_4 were higher than the *Yokelson et al.* [2003] and *Christian et al.* [2003] regressions predicted, but both of those studies examined a narrower range of higher MCEs than those achieved in FLAME. The least-squares fitting method used for the FLAME regressions was strongly influenced by the high emission factor values we observed at low MCE. The regression coefficients of the previous studies represent the data in Figure 7 for samples with fire-integrated MCE values above 0.85; our data suggest that modeled emissions from fires with lower MCE may be underpredicted by the prior-recommended EFs.

4.3.4. Carbonaceous aerosols

Elemental carbon emissions are associated with flaming-phase combustion, consistent with temperature and oxidant-dependent soot formation mechanisms. Figure 8 illustrates the relationship between fire-integrated MCE and EC/TC for emissions from two fuel classes during FLAME: needle and branch components of ponderosa pine (Figure 8a) and several chaparral and desert shrub fuels, including sagebrush, chamise, and manzanita (Figure 8b). EC/TC ratios were less than 10% for MCE values below ~0.93, and increased strongly for MCE > 0.93 for both fuel classes. The EC/TC ratio was ~0 for a sample collected during only the smoldering phase of the fire (MCE = 0.80) and 0.5 for a sample collected during the flaming phase (MCE = 0.99).

The relationships in Figure 8 were similar to previous measurements for similar fuels. *Battye and Battye* [2002] summarized recommended EF derived from a number of airborne field studies reported in the grey literature. For Ponderosa pine, EC/TC ratios for flaming / smoldering combustion were 0.06 / 0.16; for chaparral species in smoldering combustion, 0.11, whereas flaming conditions yielded 0.11-0.22. Findings from prior laboratory studies are shown in Figure

8 (*Chen et al.* [2007], *Hays et al.* [2002], *Iinuma et al*. [2007], *Christian et al.* [2003]). Note that *Hays et al.* [2002] did not report fire-integrated MCE, so we estimated fire-integrated MCE from their reported time series of Δ[CO_2] and Δ[CO] mixing ratios, and *Iinuma et al.* [2007] reported only the median and not burn-integrated values of Δ[CO] and Δ[CO_2]. Further, different techniques were used to measure EC in the various studies. Nevertheless, at similar values of MCE, the various field and laboratory measurements are in general agreement. We note that the larger range of MCE accessed in the FLAME experiments enables a better overall picture of the variations in emissions with MCE. For example, conditions with MCE~0.95 are not frequently accessible during field studies since they are associated with the intense flaming phase of combustion, but our data show that large fractions of EC can be emitted by chaparral species under those conditions. This variability over a fire lifetime may be important in estimating the final total emissions of EC to the atmosphere.

The patterns in Figure 8 were not evident for all fuels. Several produced little or no EC when burned despite featuring a substantial flaming contribution and associated high MCE. These fuels—rice straw in particular—also produced particles with some of the highest inorganic mass fractions of total $PM_{2.5}$, so it is possible the two are linked. Inorganic salts may catalyze combustion of EC on the filter during the OC-stages of the TOA, but photoacoustic measurements of the aerosol made online during the burn showed the emissions were only weakly absorbing [*Lewis et al.*, 2008], confirming the lack of EC. In their microscopy analysis of aerosol emissions, *Hopkins et al.* [2007] identified a distinct category of fuels that featured a strong flaming phase when burned, but produced a significant concentration of inorganic salts and had optical properties inconsistent with EC.

Figure 9 shows fire-integrated emission factors for OC, EC, and TC for all tested fuels as a function of fire-integrated MCE. The data are also tabulated by plant species and ecosystem in Table 2 and for each burn in Tables S2-3. A factor of 1.5 was used to compute the total organic carbon mass concentration, accounting for associated O, H, N, and other elements, from the measured C mass concentrations attributed to OC. The 1.5 factor was within the range of OM-to-OC factors of 1.4-1.8 for biomass burning aerosol recommended by *Reid et al.* [2005], and was determined appropriate for FLAME data from comparisons of reconstructed total aerosol mass concentrations with measured gravimetric mass concentrations [*Levin et al.*, in preparation].

Organic carbon emission factors were negatively correlated with MCE (r^2 = 0.36), increasing, as expected, with increasing contributions from smoldering-phase combustion (Figure 9a). Emission factors ranged from ~0.5 g C kg^{-1} fuel at high MCE to ~50 g C kg^{-1} fuel at lower MCE values. Juniper, rabbitbrush, rhododendron and white spruce were examples of plants with low OC emission factors, with emissions dominated by flaming combustion, as reflected by the fire-integrated MCE. Examples of plants with high OC emission factors included 'leafy' fuels such as kudzu, turkey oak, sagebrush, and manzanita that had low fire-integrated MCE. The coastal plain category had the highest average OC emission factor (12.4 ± 12.0 g C kg^{-1} fuel) and those in the chaparral category had the lowest (6.6 ± 10.1 g C kg^{-1} fuel), but these averages do not account for the relative abundances of particular plants in the ecosystem. The range of OC emission factors reported in the literature is very large, even for single species, as we would expect given the sensitivity of emissions to combustion conditions. OC emission factors reported for ponderosa pine range from at least 3-30 g kg^{-1} [*Hays et al.*, 2002]. *Andreae and Merlet* [2001] suggest an OC emission factor for extratropical forest fires of 8.6-9.7 g kg^{-1} fuel, somewhat lower than the averages for montane fuels we report in Table 2b, but higher than the average for boreal species.

Elemental carbon emission factors during FLAME ranged from 0–8 g C kg^{-1} fuel (Figure 9b). The significance of the relationship between EC and MCE was weaker ($r^2 = 0.11$) than that between OC and MCE. Rangeland and coastal plain species tended to have higher EC emission factors compared to fuels from other regions, but with considerable variability within the classifications. The study-average EC emission factor for montane species was 0.4 ± 0.8 g kg^{-1} fuel compared to the literature-average of 0.56 ± 0.19 reported by *Andreae and Merlet* [2001] for extratropical forests. The lower MCE in FLAME sagebrush burns, compared to those reported in *Chen et al.* [2007], led to averages of 0.63 ± 0.42 g kg^{-1} fuel compared with 1.4 g kg^{-1} fuel in that earlier study. Several studies have reported EC emission factors for ponderosa pine [e.g., *Chen et al.*, 2007; *Christian et al.*, 2003; *Hays et al.*, 2002], ranging from 0.4-2.6 g kg^{-1}, compared to 0.48 ± 0.83 g kg^{-1} in our study. *Ward and Hardy* [1991] give a range of emission factors for 'graphitic carbon' of 0.46-1.18 g kg^{-1} for fires burning in the Pacific northwest, a region with large populations of ponderosa pine.

De Gouw and Jimenez [in press] recently compared emission ratios for organic aerosols from a number of biomass burning sources, and found they range from approximately 60 to 130 μg m^{-3} (ppm ΔCO)$^{-1}$ for primary organic aerosol. The study average for FLAME was higher, at 180 ± 170 μg m^{-3} (ppm ΔCO)$^{-1}$, closer to organic aerosol / ΔCO ratios of 200 μg m^{-3} (ppm ΔCO)$^{-1}$ in an aged urban/biomass burning plume near Mexico City reported by [*DeCarlo et al.*, 2008]. Recent work by [*Grieshop et al.*, 2009] showed that biomass burning emissions can be oxidized and form secondary organic aerosol, leading to increases in the organic aerosol / ΔCO ratio, but [*Capes et al.*, 2008] did not observe any increase over fires in Africa despite other evidence of aging. The FLAME results show that high organic aerosol / ΔCO emission ratios can exist in fresh biomass burning emissions with a high level of variability, making it difficult to draw conclusions about the importance of primary and secondary sources of organic aerosol.

4.4. Nitrogen emissions

4.4.1. Gas-phase nitrogen

We compared the mass of NH_3 and NO_X emitted to the mass of N consumed in the burn, rather than to the N present in the fuel, to account for the N ash component. The NO_x measurements for FLAME 2 were estimated using measurements of NO and the mean ratio of NO_2:NO observed during FLAME 1 because an instrument malfunction prevented accurate measurement of NO_2. The N consumed by the burn was assumed to be equal to the product of the dry fuel N content and the dry mass consumed during the burn. Ammonia emissions represented approximately 21 ± 20% and nitrogen oxides represented 27 ± 26% of the N consumed, but NO_X emissions were much larger during FLAME 2 compared to FLAME 1. In FLAME 1, NH_3 and NO_X accounted for ~15% of the N consumed on average, whereas in FLAME 2 they represented ~75%. There was no strong difference in the average N contents for the fuels we burned during each of the studies, and the mass of fuel used in each burn was similar, so that fire size, as hypothesized by *Goode et al.* [1999], did not appear to be a factor. It is possible that the changes in the ignition method between the two studies may be responsible for the observed differences.

Laboratory and field measurements have shown that NO_X is emitted primarily via flaming combustion and NH_3 is emitted primarily by smoldering combustion [*Goode et al.*, 2000; *Lobert et al.*, 1991; *Yokelson et al.*, 1996]. However, emissions factors for individual nitrogen species are not strongly correlated with MCE and instead depend primarily on fuel nitrogen content [*Andreae and Merlet*, 2001; *Lobert et al.*, 1991]; *Yokelson et al.,* 2008]. To account for the fuel N dependence, *Yokelson et al.* [1996], *Goode et al.* [1999] and *Goode et al.* [2000] compared molar ratios of NH_3 and NO_x to MCE. They showed that a linear relationship between NH_3/NO_x and MCE was consistent for fire emissions measured in the laboratory and field for a variety of fuels. Figure 10 compares the *Goode et al.* [2000] relationship between NH_3/NO_X molar ratios and MCE with FLAME observations and other recently published data. The FLAME data points are shaded according to the absolute NO_X mass emissions to illustrate increasing uncertainty in the molar NH_3/NO_X ratios calculated for low NO_X cases. A linear least-squares regression to the high-NO_x data (defined as having absolute NO_X emissions greater than 0.6 g equivalent NO) indicated that NH_3 makes up the majority of the identified N emissions below a fire-integrated MCE ~0.85. Most of the samples that deviated from the linear fit corresponded to burns with low NO_X emissions and high uncertainties in the calculated NH_3/NO_X molar ratios.

NH_3/NO_X molar ratios during FLAME were about a factor of two lower than those reported and summarized by *Goode et al.* [2000] at similar MCE. *Goode et al.* [2000] treated all NO_X emissions as NO because NO_2 mixing ratios were below their instrument's detection limits. The high-NO_x FLAME data agreed with the *Goode et al.* [2000] fit if only NH_3:NO molar ratios are considered. Several other field measurements of NH_3 and NO_X from open-path and aircraft-based Fourier Transform Infrared spectrometry (FTIR) published this decade also deviated significantly from the *Goode et al.* [2000] fit, as shown in Figure 10. An improved description of NH_3/NO_X ratios in emissions may be important in estimates of global N budgets, as well as in source apportionment studies that reply on accurate profile information.

We calculated emission factors for NO, NO_2, and NH_3 following the same approach used to calculate CO, CO_2 and hydrocarbon emission factors (Table S1). Fire-integrated NO emission factors ranged from 0.04 to 9.6 g NO kg^{-1} dry fuel, with a study mean and standard deviation of 2.6 ± 2.4 g NO kg^{-1} dry fuel. There was a large difference between the average FLAME 1 EFNO (0.7 ± 0.5 g NO kg^{-1}) and the average FLAME 2 EFNO (3.9 ± 2.4 g NO kg^{-1}). This could have been due to the larger number of N-rich grasses and other plants we tested during FLAME 2. Average NO emission factors for species in the coastal plain and rangeland categories were almost three times higher than for montane and chaparral species and NH_3 emission factors were roughly 50% higher. The higher rangeland averages were due primarily to sagebrush, which had emission factors for NO and NH_3 of 5.7 ± 0.7 and 4.3 ± 1.5 g kg^{-1} fuel, respectively. The FLAME sagebrush averages are considerably higher than the EFNO of 2.94 g kg^{-1} and EFNH_3 of 0.19 g kg^{-1} reported by *Yokelson et al.* [1996].

Nitric acid (HNO_3) concentrations measured using the denuder samplers were typically much lower than the other N-containing gas species we measured. The study average emission factor was 0.02 ± 0.03 g HNO_3 kg^{-1} dry fuel, but the concentrations of HNO_3 were below the MDL for most of the samples. Nitric acid emissions were less than 1% of the N emitted in the form of NO.

4.4.2. Particulate nitrogen

We measured particulate-phase nitrogen in the form of NH_4^+, NO_3^-, and NO_2^{2-} and found that these species generally accounted for only a small fraction of the fuel nitrogen as well as a small fraction of the total $PM_{2.5}$ mass. Nitrate emission factors ranged from 0.02–0.7 g NO_3^- kg^{-1} dry fuel, with a study-average value of 0.1 ± 0.1 g kg^{-1} dry fuel. The observations span the range previously reported in the literature [*Andreae et al.*, 1998; *Hays et al.*, 2002; *Hegg et al.*, 1987]. Emissions of nitrite were lower than NO_3^- emissions by roughly a factor of two, with many samples below the MDL. Including the particulate nitrogen species, we were able to identify between 10–50% of the original fuel nitrogen, consistent with the findings of *Lobert et al.* [1990] and *Kuhlbusch et al.* [1991]. The remaining fuel nitrogen was likely emitted in the form of N_2, HCN, and nitrogen-containing organic species [*Yokelson et al.*, 2007] or remained in the ash following the burn.

4.5. Sulfur emissions

4.5.1. Sulfur dioxide

Sulfur dioxide emission factors ranged from approximately 0–1.5 g SO_2 kg^{-1} dry fuel. *Andreae and Merlet* [2001] recommended an SO_2 emission factor of 1.0 g SO_2 kg^{-1} dry fuel for extratropical forests. *Ferek et al.* [1998] observed SO_2 emission factors in the tropics ranging from roughly 0.2–1.5 g SO_2 kg^{-1} C burned, which corresponds to a range of roughly 0.1–0.7 g SO_2 kg^{-1} dry fuel assuming a fuel C fraction of 0.45. *Ferek et al.* [1998] noted that $EFSO_2$ increased weakly with MCE, but did not observe a strong correlation between MCE and $EFSO_2$, which was also not observed in our dataset.

4.5.2. Sulfate

Sulfate emission factors ranged from 0–1 g SO_4^{2-} kg^{-1} dry fuel and were weakly correlated with MCE, increasing slightly with decreasing MCE. For savanna fires in Africa, *Sinha et al.* [2003] observed sulfate emission factors on the order of 0.2 g SO_4^{2-} kg^{-1} dry fuel, whereas *Andreae et al.* [1998] reported 0.6 g SO_4^{2-} kg^{-1} dry fuel. Even higher SO_4^{2-} emission factors have been measured further from the source; e.g., the airborne data of *Andreae et al.* [1998] yielded 4–10 times higher SO_4^{2-} emission factors than did ground-based measurements closer to the fire. In our experiments, SO_2 was emitted at roughly four times the rate of SO_4^{2-}. If this emitted SO_2 is subsequently oxidized in the atmosphere to form SO_4^{2-}, the combined emission factors suggest an average yield of SO_4^{2-} of 0.7 ± 0.6 g SO_4^{2-} kg^{-1} dry fuel.

4.6. Other inorganic species

4.6.1. Chlorine

On average, chloride was the most abundant inorganic species in the aerosol during FLAME, accounting for 26 ± 16% of the soluble inorganic and 5.4 ± 7.0% of the reconstructed $PM_{2.5}$ mass concentrations. *Reid et al.* [2005] estimated Cl^- made up 2–5% of $PM_{2.5}$ in fresh biomass burning emissions and *Chen et al.* [2007] found that chloride accounted for 0.1–9.6% of $PM_{2.5}$ for several of the same fuels we burned. Emissions from several southeastern fuels burned during FLAME contained high mass fractions of chloride relative to other inorganic species. For example, chloride was ~60 % of the inorganic emissions for a palmetto leaf (*Serenoa repens*) burn.

Chloride emission factors ranged from 0.0–4.7 g kg^{-1} fuel (study average, 0.6 ± 0.8 g kg^{-1} fuel) and were not a function of MCE (Figure 9d). Previously-reported EFCl include ~0.0–3.2 g kg^{-1} fuel [*Keene et al.*, 2006]; 0.0–1.8 g kg^{-1} fuel [*Christian et al.,* 2003] and 1–2 g kg^{-1} fuel [*Andreae et al.,* 1998]. Several studies showed that roughly one-third of fuel chlorine was emitted in the form of particulate matter for tropical and savannah fuels [*Christian et al.*, 2003; *Keene et al.*, 2006; *Yokelson et al.*, 2008]. Although we did not measure the fuel chlorine content, chloride mass fractions of total inorganics within fuel classes were relatively constant, indicating that fuel type and chlorine content was the major driver of chloride emissions.

4.6.2. Potassium

Excess (non-soil and non-sea-salt) potassium has long been used as a tracer for biomass burning aerosol [*Andreae*, 1983]. It was the second-most abundant inorganic species measured during FLAME, making up 4.8 ± 5.0% of reconstructed $PM_{2.5}$ mass concentrations and 24 ± 13% of the inorganic mass. Potassium emission factors ranged from 0.0–4.7 g kg^{-1} fuel, with a study average of 0.6 ± 0.8 g kg^{-1} fuel (Figure 9e). *Christian et al.* [2003] reported EFK ranging from 0.02–1.29 g kg^{-1} for African savanna, Indonesian peat, and several wildland plant species and *Andreae and Merlet* [2001] provide literature-average values ranging from 0.08–0.41 g kg^{-1} fuel for extratropical forests. The higher values observed in FLAME were a result of the types of fuels burned. In particular, rangeland plant species had large EFK, along with many coastal plain fuels. Fire-integrated molar ratios of potassium to chloride and sulfate were consistent with K being in the form of predominately KCl with a minor contribution from K_2SO_4.

4.6.3. Other species

Sodium was 2.5 ± 3.1% of speciated fine mass on average and its mass fractions were relatively independent of fuel. Calcium, magnesium and nitrite made up the remainder of the analyzed inorganic species in the emissions. The totals of all measured inorganic emission factors were only weakly correlated with MCE ($r^2 = 0.12$) (Figure 9f), as expected since fuel composition should play the largest role in emissions of inorganic aerosol species [*Christian et al.*, 2003; *Keene et al.*, 2006].

5. DISCUSSION

The dependencies of carbonaceous and inorganic emission factors on fuel and burn characteristics have implications for predictions of biomass burning impacts on climate, air quality, and visibility, because these are sensitive to the chemical composition of the aerosol. Estimates of smoke aerosol optical properties require accurate information regarding combustion conditions in order to estimate the relative abundance of EC and OC, which to a large extent determines the single scattering albedo. Emission factors for OC and $PM_{2.5}$ are stronger functions of combustion conditions, compared to EF for inorganic compounds, but depend only weakly on plant species. Lack of data over a broad range of MCE may result in biased estimates of fire-related aerosol amounts and properties. For example, if smoldering emissions are underestimated in current biomass burning inventories, then total $PM_{2.5}$ concentrations attributable to biomass burning are likely to be underestimated: (1) the emission factors for $PM_{2.5}$ increase with decreasing MCE; (2) emissions of carbonaceous gas species increase with decreasing MCE, and it is likely that a fraction of these eventually form secondary organic aerosol; (3) as MCE decreases, more N is released in the form of NH_3, which can readily convert to particulate-phase ammonium. On-going work is examining time-resolved aerosol mass spectrometer (AMS) data obtained in the FLAME 2 studies, to examine the relationships between emissions and fire phase more closely.

There are limits to the usefulness of the MCE in capturing other effects of the fire. *Ward and Hardy* [1991] found that emission factors for total PM increased relative to $PM_{2.5}$ emissions as fire energy release rates increased. They attributed the increased PM emissions to increased turbulence for the larger fire, which lofted larger-sized PM, including ash and soil material. *Andreae et al.* [1998] observed increases in the Ca^{2+} and Mg^{2+} content of coarse mode aerosol over intense savanna fires, which they also attributed to the lofting of soil material by the turbulence in the fire. This lofting effect is not captured by the MCE, nor would the laboratory studies reproduce these soil emissions. Proxies for combustion behavior other than MCE may provide a more practical tool for linking laboratory measurements to the modeling of observed fires. For example, recent laboratory work by *Ichoku et al.* [2008] showed that fire radiative energy (FRE) measured by a thermal imaging system was strongly correlated with aerosol emission rates. This work could be extended to examine the relationships between FRE and individual gas- and particle-phase species. An advantage of FRE-based emission factors is that they can be applied to satellite measurements to develop more accurate emissions inventories.

Source apportionment techniques attempt to separate fire-related particles from other sources and to apportion the fire-related aerosols retrospectively to various fire types such as wildland, prescribed, agricultural, and residential. Most apportionment studies have been conducted using chemical transport models, receptor models, and hybrids of the two. While chemical transport models require accurate emission inventories, a necessary component of which are accurate EF, receptor-type models require appropriate tracer species to apportion sampled aerosols to these various sources. The use of a subset of FLAME data—measurements of aerosol OC, water-soluble potassium, and levoglucosan, a smoke marker compound—to develop better source profiles for biomass burning aerosols is discussed in *Sullivan et al.* [2008]. The ratios of EF we report in the Supplementary Tables for various aerosol species can also be applied as source emission profiles. For example, *Park et al.* [2007] examined observed TC-to-nonsoil-potassium ratios across the IMPROVE network to investigate the contributions by biomass burning to annual US aerosol concentrations. They estimated TC/K ratios near 10 for grassland and shrub fires in the south and ratios approaching 130 for fires in the north. We found similar ratios in the emissions from individual plant species from these regions, suggesting that our measured TC/K ratios could be used to estimate primary fire contributions to TC from the studied fuel types.

6. CONCLUSIONS

We have reported fire-integrated emission factors and aerosol mass fractions for 33 predominantly North American wildland plant species. Many, to our knowledge, have not been previously studied in laboratory open burning experiments, including the chaparral species chamise, manzanita, and ceanothus, and species common to the southeastern US (common reed, hickory, kudzu, needlegrass rush, rhododendron, cord grass, sawgrass, titi, and wax myrtle). These species frequently burn in wildland fires and prescribed burns near urban centres, so their emissions have important effects on urban air quality. We note here that the EFs reported for EC, an aerosol component that plays a key role in radiative forcing, are up to a factor of two lower than those that would be obtained if an alternate analysis protocol were used to analyze the filters, as shown by our comparisons for a limited number of burns. The magnitude of the emission factor for EC remains a significant uncertainty in estimates of the climate impacts of biomass burning.

To assist in the interpretation of our gas- and aerosol-phase measurements, we report the corresponding fire-integrated MCE. Our results are consistent with previous work that found carbonaceous gas- and particle-phase emissions depend more strongly on MCE than did the emissions of inorganic species, which depend most strongly on fuel type and composition [*Ward and Hardy*, 1991]. Combustion behavior still plays a role in the form of the inorganic emissions (e.g, NO_x vs. NH_3), but the relationships between fire-integrated inorganic gas and particle emission factors and fire-integrated MCE are weak. The aerosol composition data provide a basis set for interpreting simultaneous measurements of aerosol optical and hygroscopic properties, CCN activity, and IN activity that were conducted during FLAME.

The generally consistent relationships between laboratory- and field-derived EFs that we found in this work support the integrated approach advocated by *Yokelson et al.* [2008] for the development of more comprehensive descriptions of EFs for use in modeling. As those authors point out, different ranges of MCE are accessed in laboratory, airborne and ground-based sampling strategies, and capturing EF over a large measured range of MCE can be expected to enhance the accuracy of modeled emissions estimates. They give several examples from their own work where combining sources of data led to insights on the variation of emissions with fire phase that were not obvious from measurements over a limited range of MCE. However, two caveats in combining such data are (1) the MCE and EF we measure in the laboratory are fire-integrated, whereas those measured in a field study may represent only a portion of the burn history; and (2) the emissions in a small-scale laboratory fire do not fully reflect those in a true wildfire. Nevertheless, we have shown here, as also shown by *Yokelson et al.* [2008], that EFs for specific fuels are surprisingly consistent when interpreted through the corresponding MCE. These findings suggest value in continuing controlled laboratory studies of emissions from important fuel types that have also been observed in the field, combining the observations from various platforms and approaches to develop more robust, MCE-dependent emissions estimates.

ACKNOWLEDGEMENTS

FLAME was supported by the Joint Fire Science Program under Project JFSP 05-3-1-06, which is funded by the United States Department of Agriculture, by the National Park Service (J2350-07-5181) and by the United States Department of Energy's Office of Science (BER) through the Western Regional Center of the National Institute for Climatic Change Research. Kirchstetter was also supported by the Director, Office of Science, Office of Basic Energy Sciences, of the U.S. Department of Energy under Contract No. DE-AC02-05CH11231. We thank R. Cullin, D. Day, G. Engling, and L. Mazzoleni for their assistance in collecting samples and P. Freeborn, E. Lincoln, and the FSL staff for their help during the burns. We also thank C. McDade and L. Ashbaugh for their assistance with the IMPROVE samplers and data. FLAME fuels were provided by M. Chandler, J. Chong, D. Davis, G. Engling, G. Gonzalez, S. Grace, J. Hinkley, R. Jandt, R. Moore, S. Mucci, R. Olson, K. Outcalt, J. Reardon, K. Robertson, P.

Spaine, and D. Weise. GRM was supported by a Graduate Research Environmental Fellowship (GREF) from the United States Department of Energy’s Global Change Education Program (GCEP). The manuscript has benefited immensely from the comments of three anonymous reviewers and we thank them for their contributions.

REFERENCES

Al-Saadi, J., J. Szykman, R. B. Pierce, C. Kittaka, D. Neil, D. A. Chu, L. Remer, L. Gumley, E. Prins, L. Weinstock, C. MacDonald, R. Wayland, F. Dimmick, and J. Fishman (2005), Improving national air quality forecasts with satellite aerosol observations, *Bulletin of the American Meteorological Society*, *86*(9), 1249-+, doi:10.1175/bams-86-9-1249.

Andreae, M. O. (1983), Soot carbon and excess fine potassium - Long-range transport of combustion-derived aerosols, *Science*, *220*(4602), 1148-1151.

Andreae, M. O., T. W. Andreae, H. Annegarn, J. Beer, H. Cachier, P. le Canut, W. Elbert, W. Maenhaut, I. Salma, F. G. Wienhold, and T. Zenker (1998), Airborne studies of aerosol emissions from savanna fires in southern Africa: 2. Aerosol chemical composition, *Journal of Geophysical Research-Atmospheres*, *103*(D24), 32119-32128.

Andreae, M. O., and P. Merlet (2001), Emission of trace gases and aerosols from biomass burning, *Global Biogeochemical Cycles*, *15*(4), 955-966.

Bae, M. S., J. J. Schauer, J. T. DeMinter, J. R. Turner, D. Smith, and R. A. Cary (2004), Validation of a semi-continuous instrument for elemental carbon and organic carbon using a thermal-optical method, *Atmospheric Environment*, *38*(18), 2885-2893.

Battye, W., and R. Battye (2002), Development of emissions inventory methods for wildland fire, 91 pp, U.S. Environmental Protection Agency, Chapell Hill, NC.

Bertschi, I., R. J. Yokelson, D. E. Ward, R. E. Babbitt, R. A. Susott, J. G. Goode, and W. M. Hao (2003), Trace gas and particle emissions from fires in large diameter and belowground biomass fuels, *Journal of Geophysical Research-Atmospheres*, *108*(D13), doi:10.1029/2002JD002100.

Birch, M. E., and R. A. Cary (1996), Elemental carbon-based method for monitoring occupational exposures to particulate diesel exhaust, *Aerosol Science and Technology*, *25*(3), 221-241.

Brauer, M., P. Koutrakis, J. M. Wolfson, and J. D. Spengler (1989), Evaluation of the gas collection of an annular denuder system under simulated atmospheric conditions, *Atmospheric Environment*, *23*(9), 1981-1986.

Capes, G., B. Johnson, G. McFiggans, P. I. Williams, J. Haywood, and H. Coe (2008), Aging of biomass burning aerosols over West Africa: Aircraft measurements of chemical composition, microphysical properties, and emission ratios, *Journal of Geophysical Research-Atmospheres*, *113*(D20), doi:D00c15
10.1029/2008jd009845.

Chakrabarty, R. K., H. Moosmüller, M. A. Garro, W. P. Arnott, J. Walker, R. A. Susott, R. E. Babbitt, C. E. Wold, E. N. Lincoln, and W. M. Hao (2006), Emissions from the laboratory combustion of wildland fuels: Particle morphology and size, *Journal of Geophysical Research-Atmospheres*, *111*(D7), doi:10.1029/2005JD006659.

Chen, L. W. A., H. Moosmüller, W. P. Arnott, J. C. Chow, and J. G. Watson (2006), Particle emissions from laboratory combustion of wildland fuels: In situ optical and mass measurements, *Geophysical Research Letters*, *33*(4), 4, doi:10.1029/2005GL024838.

Chen, L. W. A., H. Moosmüller, W. P. Arnott, J. C. Chow, J. G. Watson, R. A. Susott, R. E. Babbitt, C. E. Wold, E. N. Lincoln, and W. M. Hao (2007), Emissions from laboratory combustion of wildland fuels: Emission factors and source profiles, *Environ. Sci. Technol.*, *41*(12), 4317-4325.

Chow, J. C., J. G. Watson, L. W. A. Chen, M. C. O. Chang, N. F. Robinson, D. Trimble, and S. Kohl (2007), The IMPROVE-A temperature protocol for thermal/optical carbon analysis: maintaining consistency with a long-term database, *Journal of the Air & Waste Management Association*, *57*(9), 1014-1023.

Christian, T. J., B. Kleiss, R. J. Yokelson, R. Holzinger, P. J. Crutzen, W. M. Hao, B. H. Saharjo, and D. E. Ward (2003), Comprehensive laboratory measurements of biomass-burning emissions: 1. Emissions from Indonesian, African, and other fuels, *Journal of Geophysical Research-Atmospheres*, *108*(D23), 4719, doi:10.1029/2003JD003704.

Christian, T. J., B. Kleiss, R. J. Yokelson, R. Holzinger, P. J. Crutzen, W. M. Hao, T. Shirai, and D. R. Blake (2004), Comprehensive laboratory measurements of biomass-burning emissions: 2. First intercomparison of open-path FTIR, PTR-MS, and GC- MS/FID/ECD, *Journal of Geophysical Research-Atmospheres*, *109*(D2), 12, doi:10.1029/JD2003JD003874.

Clinton, N. E., P. Gong, and K. Scott (2006), Quantification of pollutants emitted from very large wildland fires in Southern California, USA, *Atmospheric Environment*, *40*(20), 3686-3695.

Cofer, W. R., J. S. Levine, P. J. Riggan, D. I. Sebacher, E. L. Winstead, E. F. Shaw, J. A. Brass, and V. G. Ambrosia (1988a), Trace gas emissions from a mid-latitude prescribed chaparral fire, *Journal of Geophysical Research-Atmospheres*, *93*(D2), 1653-1658.

Cofer, W. R., J. S. Levine, D. I. Sebacher, E. L. Winstead, P. J. Riggin, J. A. Brass, and V. G. Ambrosia (1988b), Particulate-emissions from a mid-latitude prescribed chaparral fire, *Journal of Geophysical Research-Atmospheres*, *93*(D5), 5207-5212.

Crutzen, P. J., and M. O. Andreae (1990), Biomass burning in the tropics - Impact on atmospheric chemistry and biogeochemical cycles, *Science*, *250*(4988), 1669-1678.

de Gouw, J., and J. L. Jimenez (in press), Organic aerosols in the earth's atmosphere, *Environ. Sci. Technol.*

DeCarlo, P. F., E. J. Dunlea, J. R. Kimmel, A. C. Aiken, D. Sueper, J. Crounse, P. O. Wennberg, L. Emmons, Y. Shinozuka, A. Clarke, J. Zhou, J. Tomlinson, D. R. Collins, D. Knapp, A. J. Weinheimer, D. D. Montzka, T. Campos, and J. L. Jimenez (2008), Fast airborne aerosol size and chemistry measurements above Mexico City and Central Mexico during the MILAGRO campaign, *Atmospheric Chemistry and Physics*, *8*(14), 4027-4048.

Elliot-Fisk, D. L. (1988), The boreal forest, in *North American terrestrial vegetation*, edited by M. G. Barbour and W. D. Billings, pp. 33-62, Cambridge University Press, Cambridge.

Engling, G., P. Herckes, S. M. Kreidenweis, W. C. Malm, and J. L. Collett (2006), Composition of the fine organic aerosol in Yosemite National Park during the 2002 Yosemite Aerosol Characterization Study, *Atmospheric Environment*, *40*(16), 2959-2972.

Fine, P. M., G. R. Cass, and B. R. T. Simoneit (2001), Chemical characterization of fine particle emissions from fireplace combustion of woods grown in the northeastern United States, *Environ. Sci. Technol.*, *35*(13), 2665-2675.

Fine, P. M., G. R. Cass, and B. R. T. Simoneit (2002a), Chemical characterization of fine particle emissions from the fireplace combustion of woods grown in the southern United States, *Environ. Sci. Technol.*, *36*(7), 1442-1451.

Fine, P. M., G. R. Cass, and B. R. T. Simoneit (2002b), Organic compounds in biomass smoke from residential wood combustion: Emissions characterization at a continental scale, *Journal of Geophysical Research-Atmospheres*, *107*(D21), 9, doi:10.1029/2001JD000661.

Fine, P. M., G. R. Cass, and B. R. T. Simoneit (2004), Chemical characterization of fine particle emissions from the fireplace combustion of wood types grown in the Midwestern and Western United States, *Environmental Engineering Science*, *21*(3), 387-409.

Fites-Kaufman, J. A., P. Rundel, N. Stephenson, and D. A. Weixelman (2007), Montane and subalpine vegetation in the Sierra Nevada and Cascade ranges, in *Terrestrial vegetation of California*, edited by M. G. Barbour, et al., pp. 456-501, University of California Press, Los Angeles.

Franklin, J. F. (1988), Pacific northwest forests, in *North American terrestrial vegetation*, edited by M. G. Barbour and W. D. Billings, pp. 103-130, Cambridge University Press, Cambridge.

Freeborn, P. H., M. J. Wooster, W. M. Hao, C. A. Ryan, B. L. Nordgren, S. P. Baker, and C. Ichoku (2008), Relationships between energy release, fuel mass loss, and trace gas and aerosol emissions during laboratory biomass fires, *Journal of Geophysical Research-Atmospheres*, *113*(D1), D01301, doi:10.1029/2007JD008679.

French, N. H. F., E. S. Kasischke, and D. G. Williams (2002), Variability in the emission of carbon-based trace gases from wildfire in the Alaskan boreal forest, *Journal of Geophysical Research-Atmospheres*, *108*(D1), doi:10.1029/2001JD000480.

Friedli, H. R., E. Atlas, V. R. Stroud, L. Giovanni, T. Campos, and L. F. Radke (2001), Volatile organic trace gases emitted from North American wildfires, *Global Biogeochemical Cycles*, *15*(2), 435-452.

Goode, J. G., R. J. Yokelson, R. A. Susott, and D. E. Ward (1999), Trace gas emissions from laboratory biomass fires measured by open-path Fourier transform infrared spectroscopy: Fires in grass and surface fuels, *Journal of Geophysical Research-Atmospheres*, *104*(D17), 21237-21245.

Goode, J. G., R. J. Yokelson, D. E. Ward, R. A. Susott, R. E. Babbitt, M. A. Davies, and W. M. Hao (2000), Measurements of excess O-3, CO2, CO, CH4, C2H4, C2H2, HCN, NO, NH3, HCOOH, CH3COOH, HCHO, and CH3OH in 1997 Alaskan biomass burning plumes by airborne fourier transform infrared spectroscopy (AFTIR), *Journal of Geophysical Research-Atmospheres*, *105*(D17), 22147-22166.

Gorin, C. A., J. L. Collett, and P. Herckes (2006), Wood smoke contribution to winter aerosol in Fresno, CA, *Journal of the Air & Waste Management Association*, *56*(11), 1584-1590.

Grieshop, A. P., J. M. Logue, N. M. Donahue, and A. L. Robinson (2009), Laboratory investigation of photochemical oxidation of organic aerosol from wood fires 1: measurement and simulation of organic aerosol evolution, *Atmospheric Chemistry and Physics*, *9*(4), 1263-1277.

Haines, T. K., R. L. Busby, and D. A. Cleaves (2001), Prescribed burning in the south: trends, purpose, and barriers, *Southern Journal of Applied Forestry*, *25*(4), 149-153.

Hardy, C. C., S. G. Conard, J. C. Regelbrugge, and D. R. Teesdale (1996), Smoke emissions from prescribed burning of southern California chaparral, *Usda Forest Service Pacific Northwest Research Station Research Paper*(486), 1-&.

Hays, M. D., C. D. Geron, K. J. Linna, N. D. Smith, and J. J. Schauer (2002), Speciation of gas-phase and fine particle emissions from burning of foliar fuels, *Environ. Sci. Technol.*, *36*(11), 2281-2295.

Hegg, D. A., L. F. Radke, P. V. Hobbs, C. A. Brock, and P. J. Riggan (1987), Nitrogen and sulfur emissions from the burning of forest products near large urban areas, *Journal of Geophysical Research-Atmospheres*, *92*(D12), 14701-14709.

Hopkins, R. J., K. Lewis, Y. Desyaterik, Z. Wang, A. V. Tivanski, W. P. Arnott, A. Laskin, and M. K. Gilles (2007), Correlations between optical, chemical and physical properties of biomass burn aerosols, *Geophysical Research Letters*, *34*(18), doi:10.1029/2007GL030502.

Ichoku, C., J. V. Martins, Y. J. Kaufman, M. J. Wooster, P. H. Freeborn, W. M. Hao, S. Baker, C. A. Ryan, and B. L. Nordgren (2008), Laboratory investigation of fire radiative energy and smoke aerosol emissions, *Journal of Geophysical Research-Atmospheres*, *113*(D14), doi:10.1029/2007JD009659.

Iinuma, Y., E. Bruggemann, T. Gnauk, K. Muller, M. O. Andreae, G. Helas, R. Parmar, and H. Herrmann (2007), Source characterization of biomass burning particles: The combustion of selected European conifers, African hardwood, savanna grass, and German and Indonesian peat, *Journal of Geophysical Research-Atmospheres*, *112*(D8), 26, doi:10.1029/2006JD007120.

Jenkins, B. M., S. Q. Turn, R. B. Williams, D. P. Y. Chang, O. G. Raabe, J. Paskind, and S. Teague (1991), Quantitative assessment of gaseous and condensed phase emissions from open burning of biomass in a combustion wind-tunnel, *Global Biomass Burning*, 305-317.

Jenkins, B. M., I. M. Kennedy, S. Q. Turn, R. B. Williams, S. G. Hall, S. V. Teague, D. P. Y. Chang, and O. G. Raabe (1993), Wind-tunnel modeling of atmospheric emissions from agricultural burning - Influence of operating configuration on flame structure and particle-emission factor for a spreading-type fire, *Environ. Sci. Technol.*, *27*(9), 1763-1775.

Jenkins, B. M., A. D. Jones, S. Q. Turn, and R. B. Williams (1996), Emission factors for polycyclic aromatic hydrocarbons from biomass burning, *Environ. Sci. Technol.*, *30*(8), 2462-2469.

Kasischke, E. S., N. L. Christensen, and B. J. Stocks (1995), Fire, global warming, and the carbon balance of boreal forests, *Ecological Applications*, *5*(2), 437-451.

Kasischke, E. S., E. J. Hyer, P. C. Novelli, L. P. Bruhwiler, N. H. F. French, A. I. Sukhinin, J. H. Hewson, and B. J. Stocks (2005), Influences of boreal fire emissions on Northern Hemisphere atmospheric carbon and carbon monoxide, *Global Biogeochemical Cycles*, *19*(1), doi:10.1029/2004gb002300.

Keeley, J. E., and F. W. Davis (2007), Chaparral, in *Terrestrial vegetation of California*, edited by M. G. Barbour, et al., pp. 339-366, University of California Press, Los Angeles.

Keene, W. C., R. M. Lobert, P. J. Crutzen, J. R. Maben, D. H. Scharffe, T. Landmann, C. Hely, and C. Brain (2006), Emissions of major gaseous and particulate species during experimental burns of southern African biomass, *Journal of Geophysical Research-Atmospheres*, *111*(D4), doi:10.1029/2005JD006319.

Kirchstetter, T. W., C. E. Corrigan, and T. Novakov (2001), Laboratory and field investigation of the adsorption of gaseous organic compounds onto quartz filters, *Atmospheric Environment*, *35*(9), 1663-1671.

Kreidenweis, S. M., L. A. Remer, R. Bruintjes, and O. Dubovik (2001), Smoke aerosol from biomass burning in Mexico: Hygroscopic smoke optical model, *Journal of Geophysical Research-Atmospheres*, *106*(D5), 4831-4844.

Kuhlbusch, T. A., J. M. Lobert, P. J. Crutzen, and P. Warneck (1991), Molecular nitrogen emissions from denitrification during biomass burning, *Nature*, *351*(6322), 135-137.

Lee, T., S. M. Kreidenwels, and J. L. Collett (2004), Aerosol ion characteristics during the Big Bend Regional Aerosol and Visibility Observational Study, *Journal of the Air & Waste Management Association*, *54*(5), 585-592.

Lee, T., X. Y. Yu, B. Ayres, S. M. Kreidenweis, W. C. Malm, and J. L. Collett (2008), Observations of fine and coarse particle nitrate at several rural locations in the United States, *Atmospheric Environment*, *42*(11), 2720-2732, doi:10.1016/j.atmosenv.2007.05.016.

Levin, E. J. T., S. M. Kreidenweis, G. R. McMeeking, C. M. Carrico, J. J. L. Collett, W. C. Malm, and W. M. Hao (in preparation), FLAME refractive index and size distribution paper.

Lewis, K., W. P. Arnott, H. Moosmüller, and C. E. Wold (2008), Strong spectral variation of biomass smoke light absorption and single scattering albedo observed with a novel dual wavelength photoacoustic instrument, *Journal of Geophysical Research-Atmospheres*, doi:10.1029/2007JD009699.

Lipsky, E. M., and A. L. Robinson (2006), Effects of dilution on fine particle mass and partitioning of semivolatile organics in diesel exhaust and wood smoke, *Environ. Sci. Technol.*, *40*(1), 155-162.

Lobert, J. M., D. H. Scharffe, W. M. Hao, and P. J. Crutzen (1990), Importance of biomass burning in the atmospheric budgets of nitrogen-containing gases, *Nature*, *346*(6284), 552-554.

Lobert, J. M., D. H. Scharffe, W. M. Hao, T. A. Kuhlbusch, R. Seuwen, P. Warneck, and P. J. Crutzen (1991), Experimental evaluation of biomass burning emissions: Nitrogen and carbon containing compounds, in *Global Biomass Burning: Atmospheric, Climatic, and Biospheric Implications*, edited by J. S. Levine, pp. 289-304, MIT Press, Cambridge.

Mack, L., S. M. Kreidenweis, H. Moosmüller, J. L. Collett, C. M. Carrico, W. C. Malm, W. M. Hao, and C. E. Wold (in preparation), Optical properties of aerosols during FLAME.

Mader, B. T., and J. F. Pankow (2001), Gas/solid partitioning of semivolatile organic compounds (SOCs) to air filters. 3. An analysis of gas adsorption artifacts in measurements of atmospheric SOCs and organic carbon (OC) when using Teflon membrane filters and quartz fiber filters, *Environ. Sci. Technol.*, *35*(17), 3422-3432.

Malm, W. C., B. A. Schichtel, M. L. Pitchford, L. L. Ashbaugh, and R. A. Eldred (2004), Spatial and monthly trends in speciated fine particle concentration in the United States, *Journal of Geophysical Research-Atmospheres*, *109*(D3), 33, doi:10.1029/2003JD003739.

McMeeking, G. R., S. M. Kreidenweis, M. Lunden, J. Carrillo, C. M. Carrico, T. Lee, P. Herckes, G. Engling, D. E. Day, J. Hand, N. Brown, W. C. Malm, and J. L. Collett (2006), Smoke-impacted regional haze in California during the summer of 2002, *Agricultural and Forest Meteorology*, *137*(1-2), 25-42.

Muhle, J., T. J. Lueker, Y. Su, B. R. Miller, K. A. Prather, and R. F. Weiss (2007), Trace gas and particulate emissions from the 2003 southern California wildfires, *Journal of Geophysical Research-Atmospheres*, *112*(D3), D03307, doi:10.1029/2006JD007350.

Naeher, L. P., M. Brauer, M. Lipsett, J. T. Zelikoff, C. D. Simpson, J. Q. Koenig, and K. R. Smith (2007), Woodsmoke health effects: A review, *Inhalation Toxicology*, *19*(1), 67-106.

O'Neill, N. T., T. F. Eck, B. N. Holben, A. Smirnov, A. Royer, and Z. Li (2002), Optical properties of boreal forest fire smoke derived from Sun photometry, *Journal of Geophysical Research-Atmospheres*, *107*(D11), doi:10.1029/2001JD000877.

Obrist, D., H. Moosmüller, R. Schurmann, L. W. A. Chen, and S. M. Kreidenweis (2008), Particulate-phase and gaseous elemental mercury emissions during biomass combustion: Controlling factors and correlation with particulate matter emissions, *Environ. Sci. Technol.*, *42*(3), 721-727.

Park, R. J., D. J. Jacob, N. Kumar, and R. M. Yantosca (2006), Regional visibility statistics in the United States: Natural and transboundary pollution influences, and implications for the Regional Haze Rule, *Atmospheric Environment*, *40*(28), 5405-5423, doi:10.1016/j.atmosenv.2006.04.059.

Park, R. J., D. J. Jacob, and J. A. Logan (2007), Fire and biofuel contributions to annual mean aerosol mass concentrations in the United States, *Atmospheric Environment*, *41*, 7389-7400.

Peet, R. K. (1988), Forests of the Rocky Mountains, in *North American terrestrial vegetation*, edited by M. G. Barbour and W. D. Billings, pp. 63-101, Cambridge University Press, Cambridge.

Perrino, C., F. Desantis, and A. Febo (1990), Criteria for the choice of a denuder sampling technique devoted to the measurement of atmospheric nitrous and nitric-acids, *Atmospheric Environment Part a-General Topics*, *24*(3), 617-626.

Perrino, C., and M. Gherardi (1999), Optimization of the coating layer for the measurement of ammonia by diffusion denuders, *Atmospheric Environment*, *33*(28), 4579-4587.

Petters, M. D., M. T. Parsons, A. J. Prenni, P. J. DeMott, S. M. Kreidenweis, C. M. Carrico, A. P. Sullivan, G. R. McMeeking, E. J. T. Levin, C. E. Wold, J. J. L. Collett, and H. Moomuller (2009), Ice nuclei emissions from biomass burning, *Journal of Geophysical Research-Atmospheres*, *114*, D07209, doi:10.1029/2008JD011532.

Pfister, G. G., P. G. Hess, L. K. Emmons, P. J. Rasch, and F. M. Vitt (2008), Impact of the summer 2004 Alaska fires on top of the atmosphere clear-sky radiation fluxes, *Journal of Geophysical Research-Atmospheres*, *113*(D2), doi:10.1029/2007JD008797.

Phuleria, H. C., P. M. Fine, Y. F. Zhu, and C. Sioutas (2005), Air quality impacts of the October 2003 Southern California wildfires, *Journal of Geophysical Research-Atmospheres*, *110*(D7), doi:10.1029/2004JD004626.

Reid, J. S., R. Koppmann, T. F. Eck, and D. P. Eleuterio (2005), A review of biomass burning emissions part II: intensive physical properties of biomass burning particles, *Atmospheric Chemistry and Physics*, *5*, 799-825.

Robinson, A. L., R. Subramanian, N. M. Donahue, A. Bernardo-Bricker, and W. F. Rogge (2006), Source apportionment of molecular markers and organic aerosol. 2. Biomass smoke, *Environ. Sci. Technol.*, *40*(24), 7811-7819, doi:10.1021/es060782h.

Roden, C. A., T. C. Bond, S. Conway, A. Benjamin, and O. Pinel (2006), Emission factors and real-time optical properties of particles emitted from traditional wood burning cookstoves, *Environ. Sci. Technol.*, *40*(21), 6750-6757.

Schultz, M. G., A. Heil, J. J. Hoelzemann, A. Spessa, K. Thonicke, J. G. Goldammer, A. C. Held, J. M. C. Pereira, and M. van het Bolscher (2008), Global wildland fire emissions from 1960 to 2000, *Global Biogeochemical Cycles*, *22*(2), doi:10.1029/2007gb003031.

Spracklen, D. V., J. A. Logan, L. J. Mickley, R. J. Park, R. Yevich, A. L. Westerling, and D. A. Jaffe (2007), Wildfires drive interannual variability of organic carbon aerosol in the western U.S. in summer, *Geophysical Research Letters*, *34*, L16816, doi:10.1029/2007GL030037.

Stohl, A., E. Andrews, J. F. Burkhart, C. Forster, A. Herber, S. W. Hoch, D. Kowal, C. Lunder, T. Mefford, J. A. Ogren, S. Sharma, N. Spichtinger, K. Stebel, R. Stone, J. Strom, K. Torseth, C. Wehrli, and K. E. Yttri (2006), Pan-Arctic enhancements of light absorbing aerosol concentrations due to North American boreal forest fires during summer 2004, *Journal of Geophysical Research-Atmospheres*, *111*(D22), doi:10.1029/2006JD007216.

Sullivan, A. P., and R. J. Weber (2006), Chemical characterization of the ambient organic aerosol soluble in water: 2. Isolation of acid, neutral, and basic fractions by modified size-exclusion chromatography, *Journal of Geophysical Research-Atmospheres*, *111*(D5), doi:10.1029/2005JD006486.

Sullivan, A. P., A. S. Holden, L. A. Patterson, G. R. McMeeking, S. M. Kreidenweis, W. C. Malm, W. M. Hao, C. E. Wold, and J. L. Collett, Jr. (2008), A method for smoke marker measurements and its potential application for determining the contribution of biomass burning from wildfires and prescribed fires to ambient PM2.5 organic carbon, *Journal of Geophysical Research-Atmospheres*, *113*, D22302, doi:10.1029/2008JD010216.

Trentmann, J., G. Luderer, T. Winterrath, M. D. Fromm, R. Servranckx, C. Textor, M. Herzog, H. F. Graf, and M. O. Andreae (2006), Modeling of biomass smoke injection into the lower stratosphere by a large forest fire (Part I): reference simulation, *Atmospheric Chemistry and Physics*, *6*, 5247-5260.

Turn, S. Q., B. M. Jenkins, J. C. Chow, L. C. Pritchett, D. Campbell, T. Cahill, and S. A. Whalen (1997), Elemental characterization of particulate matter emitted from biomass burning: Wind tunnel derived source profiles for herbaceous and wood fuels, *Journal of Geophysical Research-Atmospheres*, *102*(D3), 3683-3699.

Turpin, B. J., J. J. Huntzicker, and S. V. Hering (1994), Investigation of organic aerosol sampling artifacts in the Los Angeles basin, *Atmospheric Environment*, *28*(19), 3061-3071.

van der Werf, G. R., J. T. Randerson, L. Giglio, G. J. Collatz, P. S. Kasibhatla, and A. F. Arellano (2006), Interannual variability in global biomass burning emissions from 1997 to 2004, *Atmospheric Chemistry and Physics*, *6*, 3423-3441.

Viana, M., J. M. Lopez, X. Querol, A. Alastuey, D. Garcia-Gacio, G. Blanco-Heras, P. Lopez-Mahia, M. Pineiro-Iglesias, M. Sanz, F. Sanz, X. Chi, and W. Maenhaut (2008), Tracers and impact of open burning of rice straw residues on PM in Eastern Spain, *Atmospheric Environment*, *42*(8), 1941-1957, doi:10.1016/j.atmosenv.2007.11.012.

Ward, D. E., and C. C. Hardy (1991), Smoke emissions from wildland fires, *Environment International*, *17*(2-3), 117-134.

Ward, D. E., and L. F. Radke (1993), Emission measurements from vegetation fires: a comparative evaluation of methods and results, in *Fire in the environment: the ecological, atmospheric, and climatic importance of vegetation fires*, edited by P. J. Crutzen and Goldammer, pp. 53-76, Wiley, Chichester, UK.

Watson, J. G. (2002), Visibility: Science and regulation, *Journal of the Air & Waste Management Association*, *52*(6), 628-713.

Watson, J. G., J. C. Chow, and L.-W. Antony Chen (2005), Summary of organic and elemental/black carbon analysis methods and intercomparisons, *Aerosol and Air Quality Research*, *5*(1), 65-102.

West, N. E., and J. A. Young (2000), Intermountain valleys and lower mountain slopes, in *North American terrestrial vegetation*, edited by M. G. Barbour, Cambridge University Press, Cambridge.

Wiedinmyer, C., B. Quayle, C. Geron, A. Belote, D. McKenzie, X. Y. Zhang, S. O'Neill, and K. K. Wynne (2006), Estimating emissions from fires in North America for air quality modeling, *Atmospheric Environment*, *40*(19), 3419-3432.

Yang, H. H., C. H. Tsai, M. R. Chao, Y. L. Su, and S. M. Chien (2006), Source identification and size distribution of atmospheric polycyclic aromatic hydrocarbons during rice straw burning period, *Atmospheric Environment*, *40*(7), 1266-1274.

Yokelson, R. J., D. W. T. Griffith, and D. E. Ward (1996), Open-path Fourier transform infrared studies of large-scale laboratory biomass fires, *Journal of Geophysical Research-Atmospheres*, *101*(D15), 21067-21080.

Yokelson, R. J., R. Susott, D. E. Ward, J. Reardon, and D. W. T. Griffith (1997), Emissions from smoldering combustion of biomass measured by open-path Fourier transform infrared spectroscopy, *Journal of Geophysical Research-Atmospheres*, *102*(D15), 18865-18877.

Yokelson, R. J., J. G. Goode, D. E. Ward, R. A. Susott, R. E. Babbitt, D. D. Wade, I. Bertschi, D. W. T. Griffith, and W. M. Hao (1999), Emissions of formaldehyde, acetic acid, methanol, and other trace gases from biomass fires in North Carolina measured by airborne Fourier transform infrared spectroscopy, *Journal of Geophysical Research-Atmospheres*, *104*(D23), 30109-30125.

Yokelson, R. J., T. Karl, P. Artaxo, D. R. Blake, T. J. Christian, D. W. T. Griffith, A. Guenther, and W. M. Hao (2007), The Tropical Forest and Fire Emissions Experiment: overview and airborne fire emission factor measurements, *Atmospheric Chemistry and Physics*, *7*(19), 5175-5196.

Yokelson, R. J., T. J. Christian, T. G. Karl, and A. Guenther (2008), The tropical forest and fire emissions experiment: laboratory fire measurements and synthesis of campaign data, *Atmospheric Chemistry and Physics Discussions*, *8*, 4221-4266.

Yu, X. Y., T. Lee, B. Ayres, S. M. Kreidenweis, W. Malm, and J. L. Collett (2006), Loss of fine particle ammonium from denuded nylon filters, *Atmospheric Environment*, *40*(25), 4797-4807.

TABLES

Table 1. Plant species that served as fuels during FLAME.

Common name	**Scientific name**	**Sampling location(s)**	**Carbon content (%)**	**Nitrogen content (%)**
Alaskan duff	-	Tok, Alaska	31	0.5
black spruce	*Picea mariana*	Fairbanks, AK	55	0.6
chamise	*Adenstoma fasciculatum*	San Jacinto Mountain, CA	49	1.0
common reed	*Phragmites australis*	Cameron Prairie NWR, LA	49	0.5
Douglas fir	*Pseudotsuga menziesii*	Missoula, MT	54	0.5–0.9
gallberry	*Ilex coriacea* *Ilex glabra*	Sandhill Crane NWR, MI St. Marks NWR, FL Osceola National Forest, FL	56	0.8
grass	*various species*	Missoula, MT	42	3.0
Gray’s rabbitbrush	*Ericameria nauseosa*	UT	46	1.1
hickory	*Carya nutt*	Hillsborough, NC	48	2.1
hoaryleaf ceanothus	*Ceanothus crassifolius*	San Jacinto, CA	48	1.3
kudzu	*Pueraria Montana*	Athens, GA	47	3.6
lodgepole pine	*Pinus contorta*	Missoula, MT	42–50	0.3–1.2
longleaf pine	*Pinus palustris*	North Carolina, Sandhill Crane NWR, MI St. Marks NWR, FL Camp Lejeune, NC	52	1.1
manzanita	*Arctostaphylos glandulosa*	San Jacinto, CA	48	0.8
needlegrass rush	*Juncus roemerianus*	St. Marks NWR, FL	49	1.1
palmetto	*Serenoa repens*	St. Marks NWR, FL Osceola NF, FL Sandhill Crane NWR, MS	51	1.0
peltophorum	*Peltophorum inerme*	Puerto Rico	48	0.8
ponderosa pine	*Pinus ponderosa*	Missoula, MT	46–49	0.04–1.3
Puerto Rican fern	*Dicranopteris pecitinata*	Puerto Rico	46	0.4
rhododendron	*Rhododendron minus*	-	51	0.6
rice straw	*Oryza sativa*	Douliou City, Taiwan	39–46	0.6–0.9
sagebrush	*Artemisia tridentate*	Salt Lake City, UT Missoula, MT	47–51	1.5–2.1
sea hibiscus	*Hibiscus tiliaceus*	Puerto Rico	-	-
Smooth cord grass	*Spartina alterniflora*	St. Marks NWR, FL		
sugar cane	*Saccharum officenarum*	Guangdon Province, China	48	1.3
Swamp sawgrass	*Cladium mariscus*	Big Branch Marsh NWR, LA	48	2.1
teak	*Tectona grandis*	Puerto Rico	44	0.8
titi	*Cyrilla racemiflora*	St. Marks NWR, FL	54	0.9
turkey oak	*Quercus laevis Walt.*	Hillsborough, NC Camp Lejune, NC	53	1.3
Utah juniper	*Juniperus osteosperma*	UT	49	0.9
wax myrtle	*Myrica cerifera*	Sandhill Crane NWR, FL St. Marks NWR, FL	48–53	1.1–1.4
white spruce	*Picea glauca*	Fairbanks, AK	52	0.8
wiregrass	*Aristida beyrichiana*	Sandhill Crane NWR, MS St. Marks NWR, FL Camp Lejeune, NC	48	0.5

Table 2a. Gas-phase emission factors for individual species and ecosystem groups. Emission factors are reported in g species kg^{-1} dry fuel.

Species/Group	MCE	CO_2	CO	CH_4	C_2H_4	C_3H_6	NO	NO_2	NH_3	SO_2
Montane	**0.915 ± 0.033**	**1552 ± 150**	**92.0 ± 34.1**	**3.7 ± 2.7**	**5.7 ± 4.8**	**1.7 ± 1.2**	**1.5 ± 1.9**	**0.7 ± 0.9**	**1.7 ± 1.4**	**0.4 ± 0.2**
Douglas fir	0.906 ± 0.036	1579 ± 193	106.8 ± 32.4	4.1 ± 3.8	5.8 ± 4.4	2.0 ± 1.6	3.8 ± 1.9	2.1 ± 1.0	3.3 ± 1.4	0.3 ± 0.1
lodgepole pine	0.920 ± 0.035	1528 ± 106	84.6 ± 38.8	4.2 ± 2.5	8.3 ± 7.7		0.4 ± 0.2	0.4 ± 0.3	1.3 ± 1.4	0.3 ± 0.2
Montana grass	0.863 ± 0.062	1172 ± 228	115.3 ± 50.5	4.2	8.4					
ponderosa pine	0.920 ± 0.026	1589 ± 85	88.4 ± 30.7	3.2 ± 2.0	4.4 ± 3.7	1.4 ± 0.4	0.9 ± 1.3	0.4 ± 0.2	1.3 ± 1.0	0.4 ± 0.3
Rangeland	**0.905 ± 0.043**	**1489 ± 176**	**96.4 ± 38.2**	**3.3 ± 3.1**	**3.5 ± 3.0**	**1.5 ± 1.0**	**4.6 ± 2.0**	**0.3 ± 0.2**	**2.8 ± 2.3**	**0.6 ± 0.6**
juniper	0.956	1713	51	0.2	0.7		2.2	0.2	0.4	0.1
rabbitbrush	0.935	1529	68	1.3	1.5	2.2	1.4	0.5	0.8	0.1
sagebrush	0.889 ± 0.041	1437 ± 173	111.2 ± 34.6	4.6 ± 3.1	4.4 ± 3.0	1.3 ± 1.1	5.7 ± 0.7		4.3 ± 1.5	1.0 ± 0.5
Chaparral	**0.909 ± 0.029**	**1538 ± 125**	**93.2 ± 24.1**	**2.5 ± 2.1**	**3.3 ± 2.1**	**1.4 ± 1.1**	**1.7 ± 2.2**	**0.5 ± 0.2**	**1.3 ± 1.1**	**0.3 ± 0.3**
ceanothus	0.913 ± 0.012	1623 ± 51	98.3 ± 11.6	1.7 ± 0.4	1.7 ± 0.6	0.7 ± 0.5	4.3 ± 3.9	1.1	1.5 ± 0.6	0.3 ± 0.4
chamise	0.914 ± 0.030	1562 ± 112	86.1 ± 20.9	2.3 ± 1.6	3.4 ± 2.0	1.5 ± 1.2	1.7 ± 2.2	0.4 ± 0.1	1.1 ± 0.6	0.3 ± 0.3
manzanita	0.899 ± 0.030	1471 ± 138	104.4 ± 28.9	3.8 ± 3.6	4.1 ± 3.0	1.9 ± 1.3	1.3 ± 1.8	0.5 ± 0.1	1.8 ± 1.9	0.2 ± 0.1
Coastal plain	**0.930 ± 0.029**	**1632 ± 150**	**78.0 ± 27.7**	**2.7 ± 1.7**	**2.6 ± 2.2**	**1.1 ± 1.2**	**4.5 ± 2.4**	**0.7 ± 0.4**	**2.0 ± 1.2**	**0.5 ± 0.5**
black needlerush	0.891 ± 0.030	1538 ± 114	119.0 ± 28.3	5.4 ± 1.8	4.1 ± 1.7	0.7	3.8 ± 0.3		1.8	0.7
common reed	0.957 ± 0.013	1656 ± 9	47.0 ± 15.6	1.6 ± 0.4	2.7 ± 0.0		8.1 ± 2.1		1.7	
gallberry	0.947 ± 0.004	1868 ± 5	66.0 ± 4.2	2.4 ± 0.2	1.7 ± 0.2	0.5 ± 0.0	7.3		1.9	
hickory	0.933 ± 0.005	1583 ± 24	72.0 ± 4.2	2.7 ± 0.5	1.9 ± 0.1	0.5 ± 0.0			3.5	
kudzu	0.857 ± 0.003	1096 ± 35	116.5 ± 0.7	4.8 ± 1.7	8.4 ± 1.0	2.3 ± 0.2	6.5 ± 1.2			
longleaf pine	0.944 ± 0.023	1659 ± 78	60.8 ± 27.6	2.1 ± 0.9	2.7 ± 3.4	1.6 ± 2.2	3.2 ± 1.5	1.3	2.2 ± 0.8	0.0 ± 0.0
oak	0.943 ± 0.007	1622 ± 43	65.7 ± 3.5	1.7 ± 0.6	2.4 ± 0.4	0.6 ± 0.2	9.6		3.8	
palmetto	0.933 ± 0.018	1678 ± 65	75.9 ± 19.5	2.3 ± 1.6	1.5 ± 0.8	0.6 ± 0.4	2.9 ± 1.9	0.5 ± 0.2	1.0 ± 0.8	0.8 ± 0.5
rhododendron	0.961	1783	46	1.8	1.2		3.9		2.2	0.1
sawgrass	0.900 ± 0.008	1522 ± 16	107.0 ± 8.5	3.4 ± 0.0	2.0 ± 0.2		5.9 ± 0.6		2.5	1.1
titi	0.942	1825	71	1.8	1.1		7.6			
turkey oak	0.886 ± 0.006	1580 ± 31	129.5 ± 4.9	5.9 ± 1.2	4.3 ± 0.8	1.4 ± 0.3	6.3 ± 0.2		5.3	0.7
wax myrtle	0.915 ± 0.013	1622 ± 61	95.7 ± 11.5	2.9 ± 0.9	3.7 ± 2.7	2.0 ± 2.3	3.6 ± 3.7	1	2.2 ± 0.7	0
wire grass	0.965 ± 0.007	1680 ± 9	43.0 ± 1.4	0.6 ± 0.2	0.4 ± 0.1	0.2	3.5 ± 0.4		0.6	
Boreal forest	**0.917 ± 0.068**	**1311 ± 325**	**70.6 ± 40.2**	**1.4 ± 0.9**	**1.7 ± 1.6**	**0.7 ± 0.6**	**3.3 ± 1.8**	**1.6 ± 1.1**	**1.8 ± 1.1**	**0.1 ± 0.1**
Alaskan duff	0.867 ± 0.074	1034 ± 175	96.4 ± 43.0	2.3 ± 0.9	2.5 ± 2.7	1.1 ± 1.0	2.0 ± 0.7	1.0 ± 0.5	2.3 ± 1.2	0.1 ± 0.1
black spruce	0.957 ± 0.012	1588 ± 125	44.8 ± 11.2	0.8 ± 0.4	1.3 ± 0.4	0.5 ± 0.3	3.9 ± 2.0	3.2	1.1 ± 0.6	0.1
white spruce	0.971			1.7					2.5	0.2
Other	**0.922 ±**	**1411 ±**	**84.4 ±**	**2.8 ± 2.8**	**2.0 ± 2.0**	**0.8 ± 0.7**	**2.2 ± 2.1**	**0.5 ± 0.1**	**0.8 ± 0.6**	**0.4 ± 0.4**

	0.035	**82**	**29.8**							
fern	0.943	1571	60	1.7	2.3	2.1	0.8	0.5	0.7	0
PR mixed woods	0.952			1.7	0.8	0.8				
rice straw	0.911 ± 0.032	1394 ± 64	87.1 ± 30.3	3.6 ± 3.3	2.4 ± 2.4	0.5 ± 0.3	2.5 ± 2.2	0.4 ± 0.0	0.8 ± 0.6	0.5 ± 0.4
sugar cane	0.977			0.8	0.9					

Table 2b. Aerosol-phase emission factors by ecosystem species and group.

Species/Group	**MCE**	**OC**	**EC**	**K^+**	**Na^+**	**NH_4^+**	**Cl^-**	**NO_3^-**	**SO_4^{2-}**	**$PM_{2.5}$**
Montane	**0.915 ± 0.033**	**18.4 ± 16.3**	**0.4 ± 0.8**	**0.3 ± 0.7**	**0.3 ± 0.6**	**0.3 ± 0.3**	**0.2 ± 0.2**	**0.1 ± 0.1**	**0.1 ± 0.1**	**29.4 ± 25.1**
Douglas fir	0.906 ± 0.036	26.0 ± 14.9	0.36 ± 0.75	0.90 ± 1.22	0.79 ± 1.21	0.50 ± 0.38	0.31 ± 0.40	0.22 ± 0.19	0.32 ± 0.05	42.9 ± 22.9
lodgepole pine	0.920 ± 0.035	11.3 ± 15.2	0.45 ± 0.70	0.12 ± 0.19	0.11 ± 0.07	0.12 ± 0.04	0.13 ± 0.10	0.12 ± 0.05	0.08 ± 0.07	18.1 ± 23.1
Montana grass	0.863 ± 0.062									
ponderosa pine	0.920 ± 0.026	17.6 ± 17.0	0.48 ± 0.83	0.14 ± 0.27	0.17 ± 0.26	0.15 ± 0.14	0.14 ± 0.13	0.08 ± 0.05	0.06 ± 0.06	27.7 ± 26.0
Rangeland	**0.905 ± 0.043**	**9.4 ± 8.1**	**1.2 ± 0.9**	**1.3 ± 0.9**	**0.4 ± 0.4**	**0.6 ± 0.5**	**1.2 ± 1.2**	**0.0 ± 0.0**	**0.2 ± 0.2**	**18.9 ± 13.9**
juniper	0.956	0.7	2.7	0.2	0.02	0.31	0.11	0.01	0.08	4.2
rabbitbrush	0.935	0.5	1.4	0.67	0.03	0.23	0.28	0.06	0.18	3.4
sagebrush	0.889 ± 0.041	15.3 ± 1.2	0.63 ± 0.42	1.83 ± 0.67	0.61 ± 0.22	0.83 ± 0.57	1.82 ± 1.08		0.43	29.0 ± 1.9
Chaparral	**0.909 ± 0.029**	**6.6 ± 10.1**	**0.5 ± 0.4**	**0.4 ± 0.3**	**0.2 ± 0.2**	**0.5 ± 0.5**	**0.2 ± 0.1**	**0.2 ± 0.1**	**0.2 ± 0.1**	**11.6 ± 15.1**
ceanothus	0.913 ± 0.012	3.8 ± 0.1	0.35 ± 0.35	0.60 ± 0.40	0.09 ± 0.09	0.11	0.38 ± 0.13	0.11	0.31 ± 0.20	7.8 ± 1.2
chamise	0.914 ± 0.030	3.2 ± 2.5	0.56 ± 0.48	0.38 ± 0.29	0.17 ± 0.23	0.50 ± 0.46	0.20 ± 0.14	0.15 ± 0.08	0.17 ± 0.07	6.5 ± 4.2
manzanita	0.899 ± 0.030	14.8 ± 17.3	0.35 ± 0.31	0.27 ± 0.14	0.16 ± 0.13	0.50 ± 0.70	0.16 ± 0.07	0.16 ± 0.07	0.16 ± 0.10	23.5 ± 25.9
Coastal plain	**0.930 ± 0.029**	**12.4 ± 12.0**	**0.9 ± 1.7**	**0.8 ± 1.1**	**0.4 ± 0.5**	**0.6 ± 0.6**	**1.2 ± 1.2**	**0.1 ± 0.1**	**0.3 ± 0.2**	**23.4 ± 18.7**
black needlerush	0.891 ± 0.030	18.3	0.3	3.19	2.06	0.57 ± 0.75	4.73		0.49	38.4
common reed	0.957 ± 0.013	19.7	0.4	1.08	0.98	0.38	2.54			36.2
gallberry	0.947 ± 0.004	7.1	8.1	0.61	0.16		0.16		0.45	20.5
hickory	0.933 ± 0.005	7.1	0.3	0.46	0.24		0.23			12.5
kudzu	0.857 ± 0.003	44.2	0	1.06	0.65	0.45	0.39		0.99	70.5
longleaf pine	0.944 ± 0.023	23.8 ± 8.9	0.93 ± 0.32	0.24 ± 0.12	0.16 ± 0.06	0.62 ± 0.59	0.85 ± 0.44	0.02	0.14 ± 0.01	38.3 ± 13.6
oak	0.943 ± 0.007	10.6	0.4	0.54	0.28	0.51	0.23		0.4	18.2
palmetto	0.933 ± 0.018	5.0 ± 6.6	0.47 ± 0.34	0.47 ± 0.45	0.16 ± 0.08	0.52 ± 0.46	1.27 ± 0.55	0.10 ± 0.10	0.20 ± 0.12	11.4 ± 10.5
rhododendron	0.961	2.1	0.2	0.08	0.03	0.32	0.08		0.04	3.7
sawgrass	0.900 ± 0.008	9.2	1.1	4.69	0.68	1.32	3.87		0.35	24.6
titi	0.942									

turkey oak	0.886 ± 0.006	32.5	1.4	1.01	0.37	2.06	0.33		0.23	52.2
wax myrtle	0.915 ± 0.013	6.3 ± 2.5	0.35 ± 0.07	0.62 ± 0.06	0.28 ± 0.01	0.06	0.95 ± 0.25	0.08	0.26 ± 0.13	12.2 ± 4.0
wire grass	0.965 ± 0.007	3.5	0.3	0.19	0.17	0.87	0.18	0.1		6.4
Boreal forest	**0.917 ± 0.068**	**7.8 ± 7.2**	**0.2 ± 0.4**	**0.2 ± 0.1**	**0.2 ± 0.4**	**0.5 ± 0.8**	**0.1 ± 0.2**	**0.1 ± 0.1**	**0.0 ± 0.0**	**12.7 ± 11.3**
Alaskan duff	0.867 ± 0.074	10.2 ± 10.0	0.00 ± 0.00	0.15 ± 0.19	0.32 ± 0.54	0.26	0.14 ± 0.22	0.04 ± 0.01	0.05 ± 0.01	16.1 ± 15.9
black spruce	0.957 ± 0.012	6.2 ± 2.8	0.60 ± 0.46	0.15 ± 0.10	0.09 ± 0.05	0.84 ± 1.11	0.10 ± 0.07	0.16	0.04	10.4 ± 4.2
white spruce	0.971	3.5	0	0.16	0.08	0.01	0.31	0.1		5.9
Other	**0.922 ± 0.035**	**5.6 ± 3.5**	**0.1 ± 0.1**	**0.5 ± 0.3**	**0.1 ± 0.1**	**0.3 ± 0.6**	**1.0 ± 0.5**	**0.1 ± 0.0**	**0.1 ± 0.1**	**10.2 ± 6.6**
fern	0.943	2.2	0.1	0.06	0.01	0.1	0.01	0.04	0.04	3.9
PR mixed woods	0.952					0.09		0.01		
rice straw	0.911 ± 0.032	6.2 ± 3.5	0.08 ± 0.15	0.57 ± 0.18	0.14 ± 0.13	0.44 ± 0.72	1.19 ± 0.15	0.08 ± 0.02	0.12 ± 0.09	11.8 ± 6.5
sugar cane	0.977					0.1		0.07		

FIGURE CAPTIONS

Figure 1. Schematic of the US Forest Service Fire Sciences Laboratory combustion facility, located in Missoula, Montana. Image is to scale. The locations of the fuel bed and of the sampling ports during stack and chamber burns are indicated.

Figure 2. Scatter plots comparing elemental carbon (EC) concentrations normalized by total aerosol carbon (TC) concentrations, for each thermal optical analysis protocol and/or filter sampler used during FLAME chamber burns. The dashed black line is the 1:1 line and the two dashed gray lines are the 1:2 and 2:1 lines.

Figure 3. Organic carbon (OC) concentrations measured on the back IMPROVE quartz filter normalized by OC measured on the front IMPROVE quartz filter, as a function of front filter OC. Chamber burns only.

Figure 4. Fire-integrated modified combustion efficiency plotted as a function of fuel moisture (in dry weight %).

Figure 5. Gravimetrically-determined mass concentrations of particles with aerodynamic diameters less than 10 μm (PM_{10}) compared to gravimetrically-determined mass concentrations of particles with diameters less than 2.5 μm ($PM_{2.5}$) for IMPROVE filter samples obtained during chamber burns. Dashed line is the 1:1 line. Solid line gives the linear regression of PM_{10} mass onto $PM_{2.5}$ mass, forced through the origin, for all but the highest three concentration samples.

Figure 6. Carbon mass consumed versus carbon mass emitted during FLAME. Carbon mass consumed was calculated assuming the residual mass had zero water content. Carbon mass

emitted consists of the sum of carbon monoxide, carbon dioxide, methane, $C_{2\text{-}4}$ hydrocarbons, and particulate carbon. Points are shaded by fuel moisture to indicate samples where the assumption is less likely to be valid. Circles indicate stack burns and triangles indicate chamber burns.

Figure 7. Fire-integrated emission factors for hydrocarbon gas species calculated from canister gas chromatography measurements as a function of fire-integrated modified combustion efficiency (MCE), for all tested fuels. Black lines indicate the linear least-squares regression of the emission factors onto MCE.

Figure 8. Elemental-to-total aerosol carbon (EC/TC) ratios observed for emissions from (a) ponderosa pine and (b) chaparral and desert shrub fuels, versus fire-integrated modified combustion efficiency (MCE). Ponderosa pine data include needle, branch, needles and branches, needle litter and duff burns. Samples collected during only flaming (high MCE) and smoldering (low MCE) combustion of ponderosa pine needles are indicated by the filled circles; all others are fire-integrated. Previously measured ratios from selected studies are also shown.

Figure 9. Fire-integrated aerosol emission factors (EF) as a function of fire-integrated modified combustion efficiency (MCE) for: a) organic carbon (OC); b) elemental carbon (EC); c) total aerosol carbon (TC); d) chloride; e) potassium; f) total inorganic aerosol species and g) reconstructed PM2.5. Black lines indicate the linear regression of EF onto MCE with coefficients and coefficient of variation indicated on the plot for each species.

Figure 10. Molar ratios of NH_3-to-NO_X emissions as a function of fire-integrated modified combustion efficiency (MCE) during FLAME and as reported for several other biomass burning field and laboratory experiments, as indicated in the legend. FLAME data are shaded to reflect

the magnitude of the NO_X measurement, and therefore reflect the confidence in the measured ratio. The dashed line indicates the fit provided by *Goode et al.* [2000] for several sets of laboratory and field biomass burning measurements. Note that this figure is truncated to better illustrate the majority of NH_3/NO_X data from our study and the literature. A maximum $NH_3:NO_X$ ratio of ~12 at an MCE of 0.82 was reported by *Christian et al.* [2003].

FIGURES

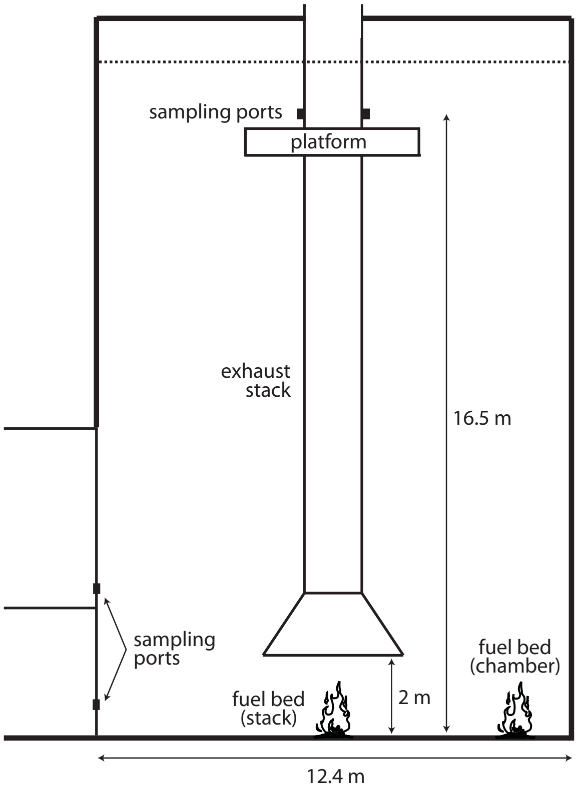

Figure 1 Schematic of the US Forest Service Fire Sciences Laboratory combustion facility, located in Missoula, Montana. Image is to scale. The locations of the fuel bed and of the sampling ports during stack and chamber burns are indicated.

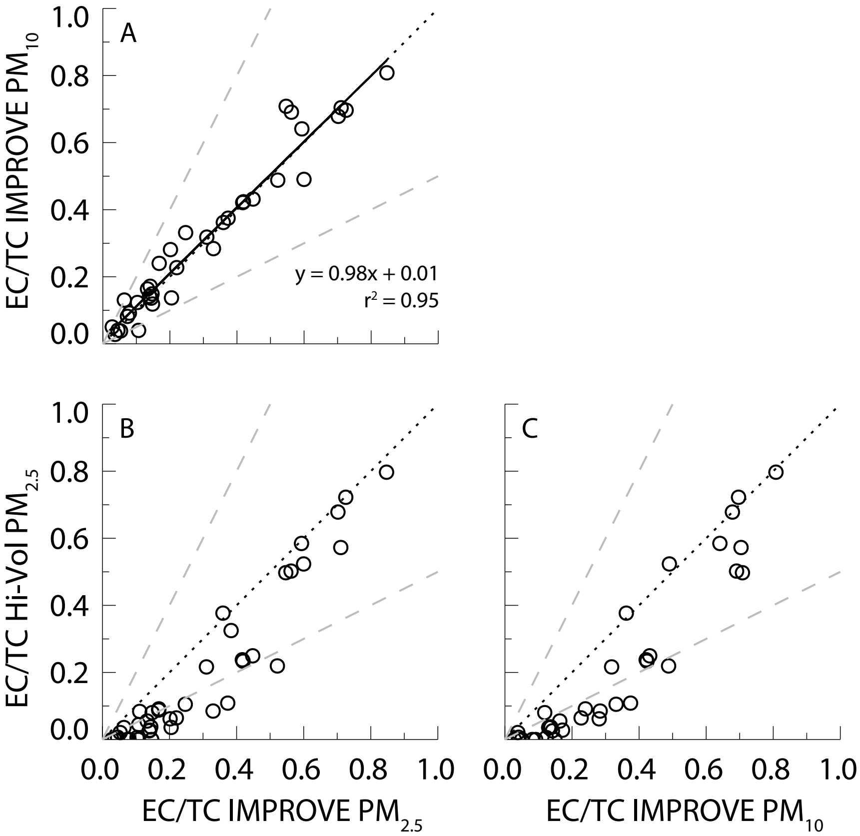

Figure 2 Scatter plots comparing elemental carbon (EC) concentrations normalized by total aerosol carbon (TC) concentrations, for each thermal optical analysis protocol and/or filter sampler used during FLAME chamber burns. The dashed black line is the 1:1 line and the two dashed gray lines are the 1:2 and 2:1 lines.

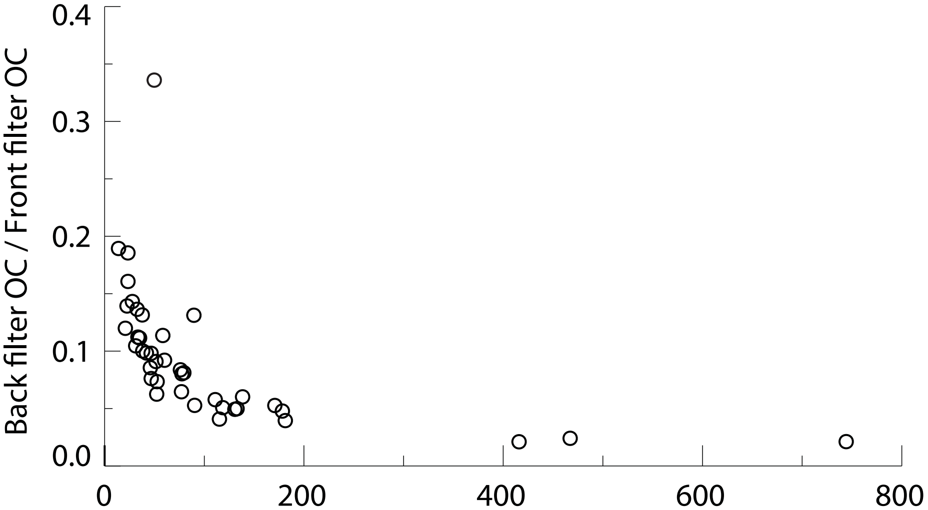

Figure 3 Organic carbon (OC) concentrations measured on the back IMPROVE quartz filter normalized by OC measured on the front IMPROVE quartz filter, as a function of front filter OC. Chamber burns only.

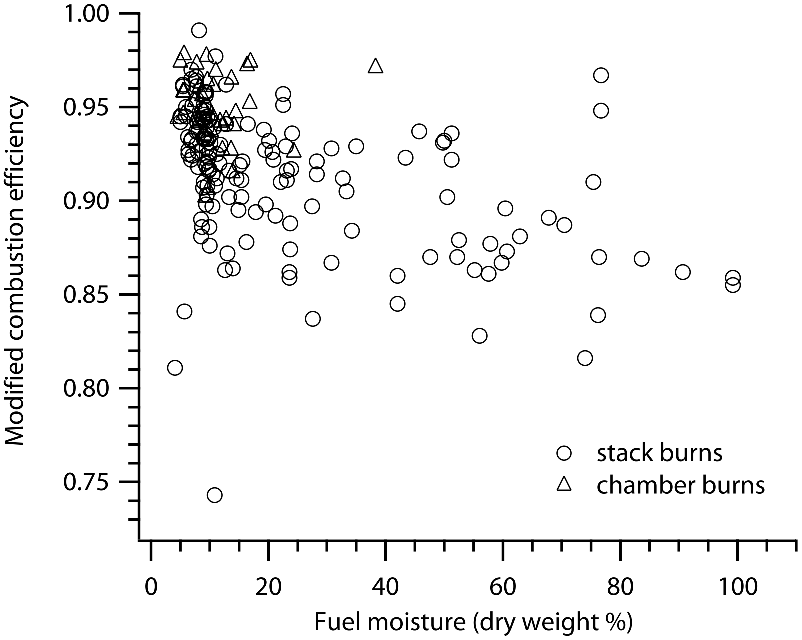

Figure 4 Fire-integrated modified combustion efficiency plotted as a function of fuel moisture (in dry weight %).

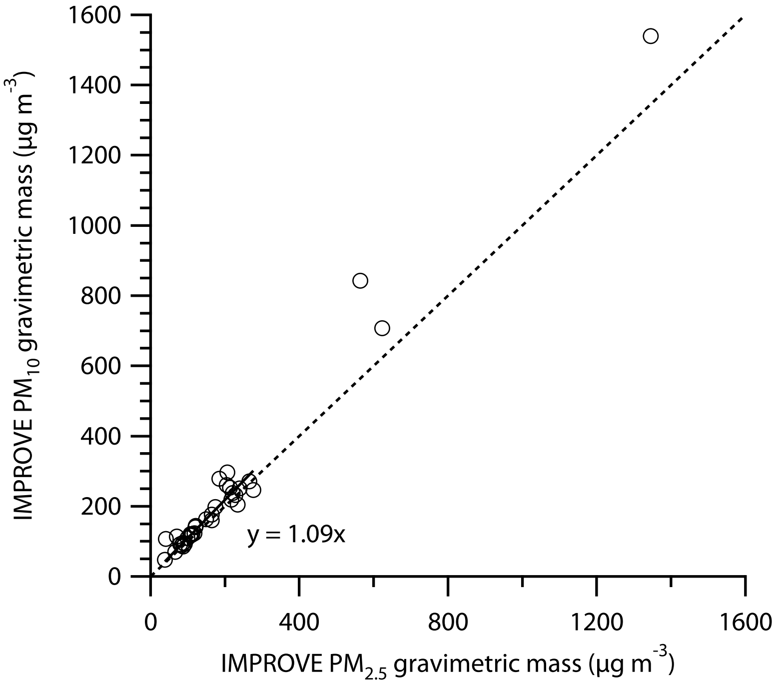

Figure 5 Gravimetrically-determined mass concentrations of particles with aerodynamic diameters less than 10 µm (PM_{10}) compared to gravimetrically-determined mass concentrations of particles with diameters less than 2.5 µm ($PM_{2.5}$) for IMPROVE filter samples obtained during chamber burns. Dashed line is the 1:1 line. Solid line gives the linear regression of PM_{10} mass onto $PM_{2.5}$ mass, forced through the origin, for all but the highest three concentration samples.

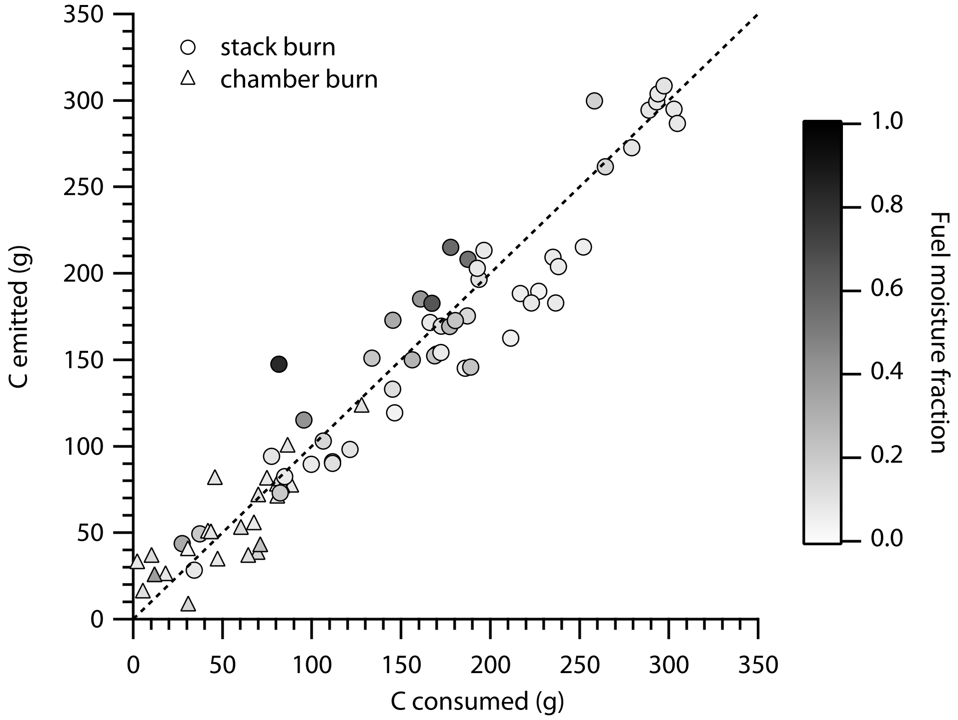

Figure 6 Carbon mass consumed versus carbon mass emitted during FLAME. Carbon mass consumed was calculated assuming the residual mass had zero water content. Carbon mass emitted consists of the sum of carbon monoxide, carbon dioxide, methane, C_{2-4} hydrocarbons, and particulate carbon. Points are shaded by fuel moisture to indicate samples where the assumption is less likely to be valid. Circles indicate stack burns and triangles indicate chamber burns.

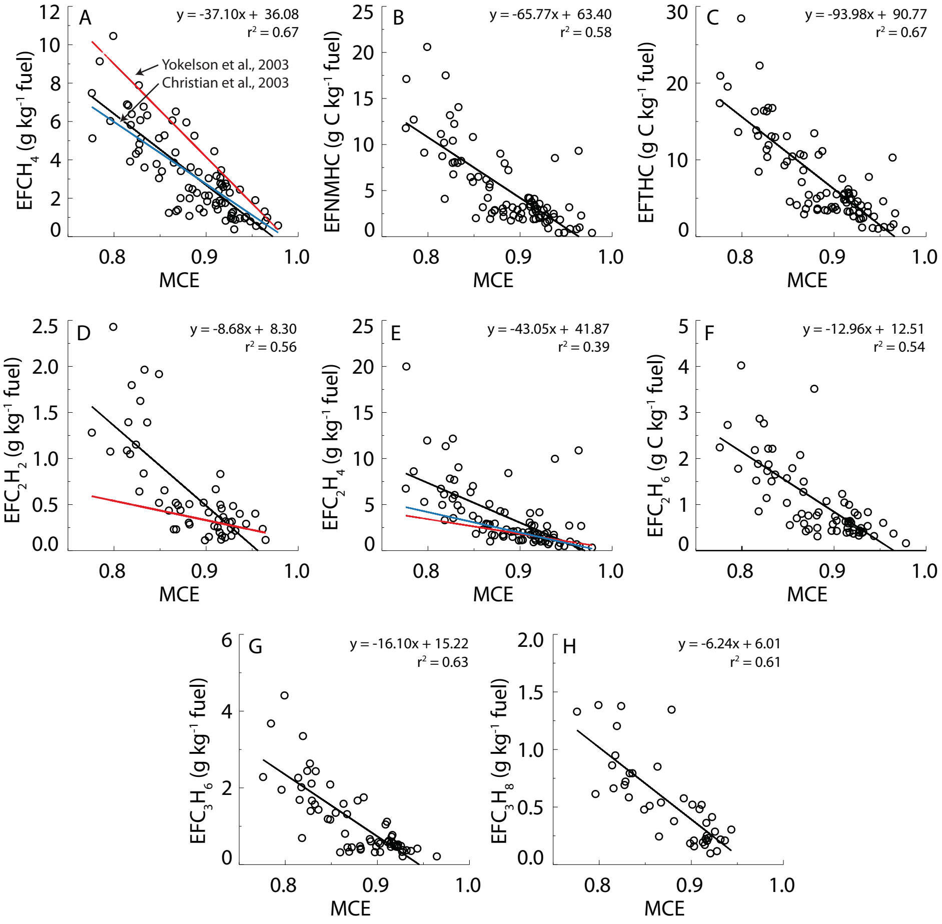

Figure 7 Fire-integrated emission factors for hydrocarbon gas species calculated from canister gas chromatography measurements as a function of fire-integrated modified combustion efficiency (MCE), for all tested fuels. Black lines indicate the linear least-squares regression of the emission factors onto MCE.

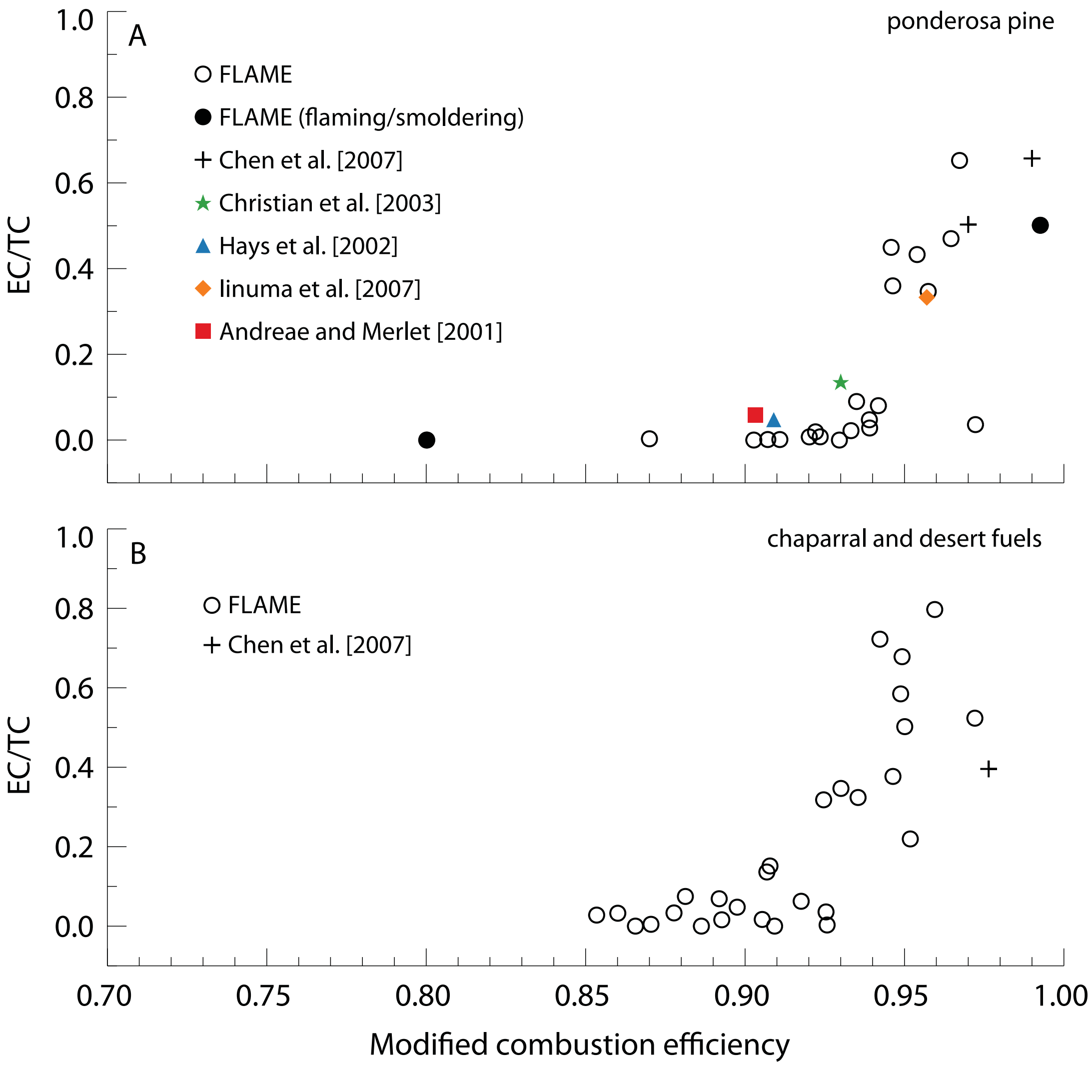

Figure 8 Elemental-to-total aerosol carbon (EC/TC) ratios observed for emissions from (a) ponderosa pine and (b) chaparral and desert shrub fuels, versus fire-integrated modified combustion efficiency (MCE). Ponderosa pine data include needle, branch, needles and branches, needle litter and duff burns. Samples collected during only flaming (high MCE) and smoldering (low MCE) combustion of ponderosa pine needles are indicated by the filled circles; all others are fire-integrated. Previously measured ratios from selected studies are also shown.

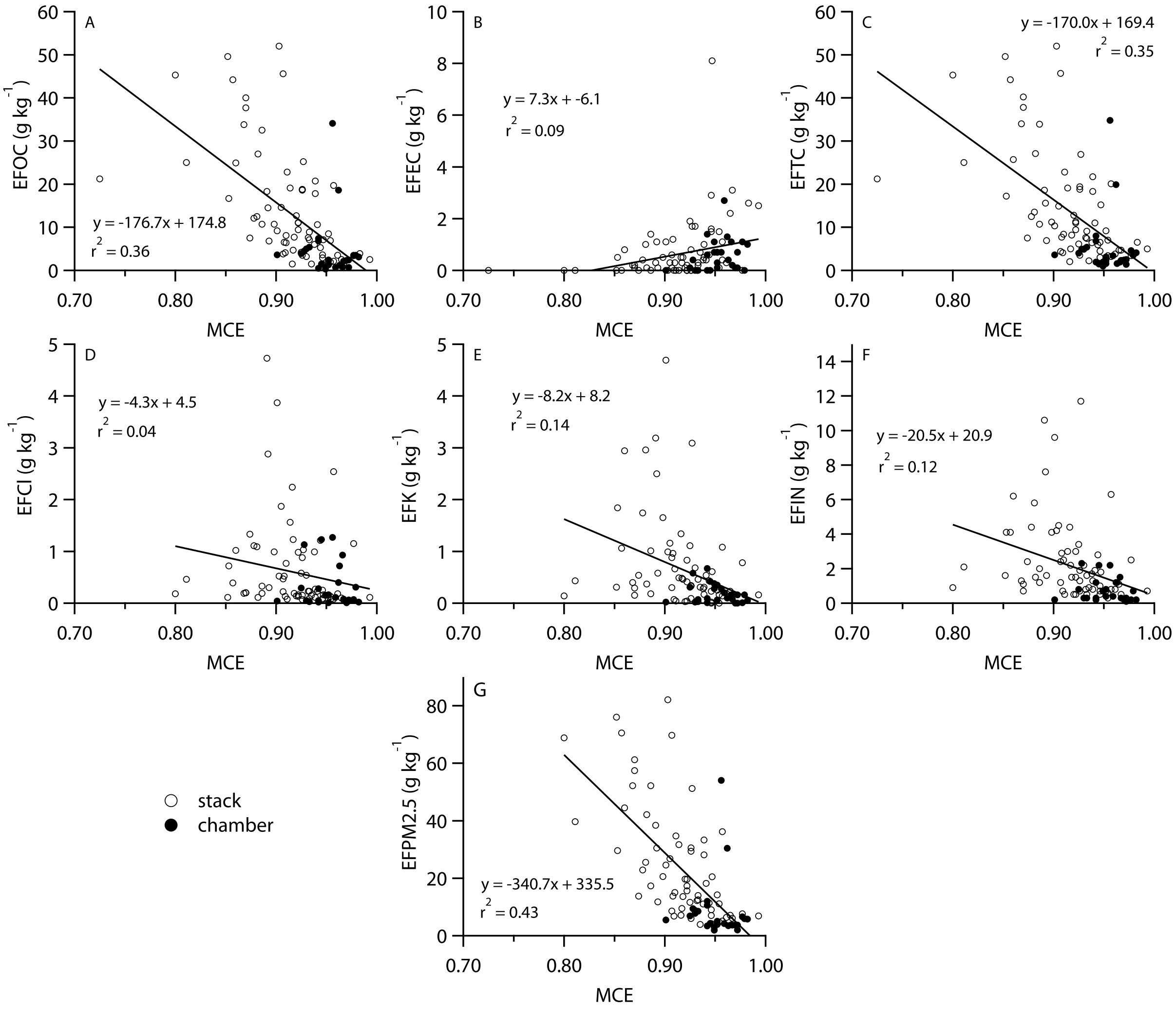

Figure 9 Fire-integrated aerosol emission factors (EF) as a function of fire-integrated modified combustion efficiency (MCE) for: a) organic carbon (OC); b) elemental carbon (EC); c) total aerosol carbon (TC); d) chloride; e) potassium; f) total inorganic aerosol species and g) reconstructed PM2.5. Black lines indicate the linear regression of EF onto MCE with coefficients and coefficient of variation indicated on the plot for each species.

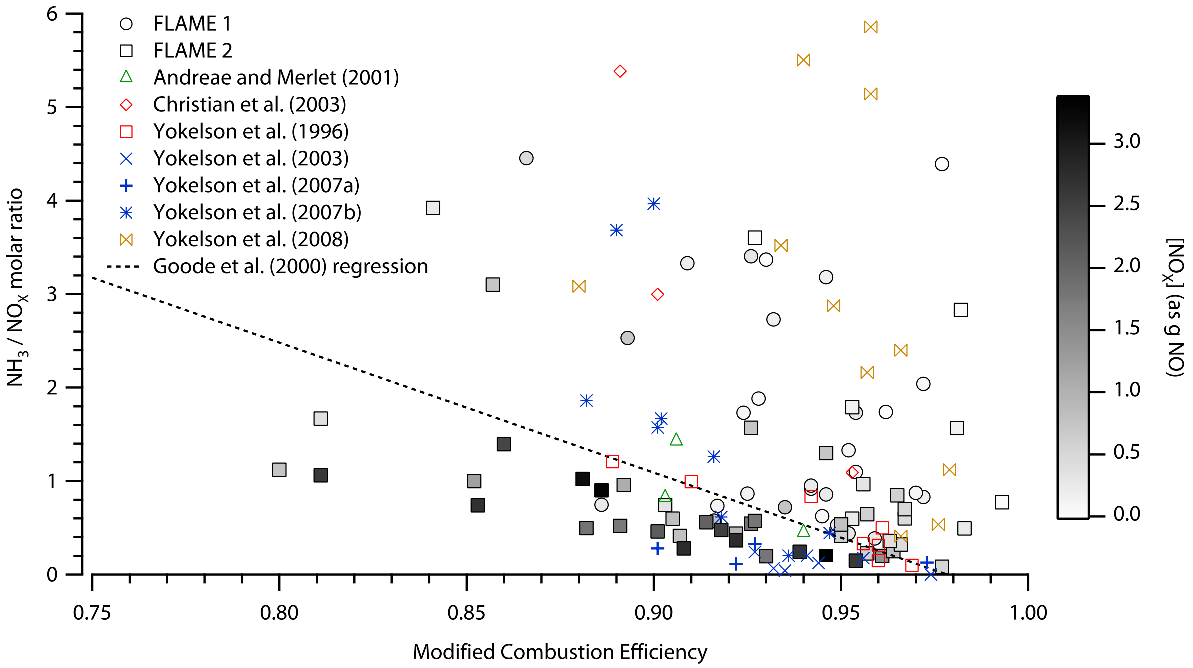

Figure 10 Molar ratios of NH_3-to-NO_X emissions as a function of fire-integrated modified combustion efficiency (MCE) during FLAME and as reported for several other biomass burning field and laboratory experiments, as indicated in the legend. FLAME data are shaded to reflect the magnitude of the NO_X measurement, and therefore reflect the confidence in the measured ratio. The dashed line indicates the fit provided by *Goode et al.* [2000] for several sets of laboratory and field biomass burning measurements. Note that this figure is truncated to better illustrate the majority of NH_3/NO_X data from our study and the literature. A maximum NH_3:NO_X ratio of ~12 at an MCE of 0.82 was reported by *Christian et al.* [2003].